Cell Calcium 71 (2018) 1–14

Contents lists available at ScienceDirect

Cell Calcium

journal homepage: www.elsevier.com/locate/ceca

Coupling of P2Y receptors to Ca^{2+} mobilization in mesenchymal stromal cells from the human adipose tissue

Polina D. Kotova[a], Marina F. Bystrova[a], Olga A. Rogachevskaja[a], Alexander A. Khokhlov[a], Veronika Yu. Sysoeva[b], Vsevolod A. Tkachuk[b], Stanislav S. Kolesnikov[a,*]

[a] Institute of Cell Biophysics, Russian Academy of Sciences, Institutional Street 3, Pushchino, Moscow Region, 142290, Russia
[b] Department of Biochemistry and Molecular Medicine, Faculty of Basic Medicine, Lomonosov Moscow State University, Russia

ARTICLE INFO

Keywords:
Purinoreceptors
Calcium-induced calcium release
IP_3 receptors
Mesenchymal stromal cells
Adipose tissue

ABSTRACT

The purinergic transduction was examined in mesenchymal stromal cells (MSCs) from the human adipose tissue, and several nucleotides, including ATP, UTP, and ADP, were found to mobilize cytosolic Ca^{2+}. Transcripts for multiple purinoreceptors were detected in MSC preparations, including A_1, A_{2A}, A_{2B}, $P2Y_1$, $P2Y_2$, $P2Y_4$, $P2Y_6$, $P2Y_{11}$, $P2Y_{13}$, $P2Y_{14}$, $P2X_2$, $P2X_4$, and $P2X_7$. Cellular responses to nucleotides were insignificantly sensitive to bath Ca^{2+}, pointing at a minor contribution of Ca^{2+} entry, and were suppressed by U73122 and 2-APB, implicating the phosphoinositide cascade in coupling P2Y receptors to Ca^{2+} release. While individual cells were sensitive to several P2Y agonists, responsiveness to a given nucleotide varied from cell to cell, suggesting that particular MSCs could employ different sets of purinoreceptors. Caged Ca^{2+} stimulated Ca^{2+}-induced Ca^{2+} release (CICR) that was mediated largely by IP_3 receptors, and resultant Ca^{2+} transients were similar to nucleotide responses by magnitude and kinetics. A variety of findings hinted at CICR to be a universal mechanism that finalizes Ca^{2+} signaling initiated by agonists in MSCs. Individual MSCs responded to nucleotides in an all-or-nothing manner. Presumably just CICR provided invariant Ca^{2+} responses observed in MSCs at different nucleotide concentrations. The effects of isoform specific agonists and antagonists suggested that both $P2Y_1$ and $P2Y_{13}$ were obligatory for ADP responses, while $P2Y_4$ and $P2Y_{11}$ served as primary UTP and ATP receptors, respectively. Extracellular NAD^+ stimulated Ca^{2+} signaling in each ATP-responsive MSC by involving $P2Y_{11}$. The overall data indicate that extracellular nucleotides and NAD^+ can serve as autocrine/paracrine factors regulating MSC functions.

1. Introduction

Cells-to-cell communications and autocrine regulations are mediated by a variety of signaling molecules that are released into and diffuse within the extracellular space to hit on multiple cell surface receptors coupled to intracellular signaling or regulatory processes. Among them, purines (ATP, ADP, β-NAD, ADPR, cADPR, and adenosine) and pyrimidines (UTP and UDP) are released by cells or produced extracellularly by ecto-nucleotidases in virtually all tissues [1–3]. The responsiveness to purines and pyrimidines is widespread among eukaryotic cells, which express numerous purinoreceptors from the P1 and P2 families. The P1 subgroup includes four G-protein-coupled receptors (A_1, A_{2A}, A_{2B}, A_3) recognizing adenosine as an endogenous agonist [4], while the more diverse P2 family is composed of ionotropic P2X and metabotropic P2Y receptors. P2X receptors are cationic channels specifically gated by ATP, while P2Y receptors are activated by multiple purine and pyrimidine nucleotides or by sugar-nucleotides and couple to intracellular second-messenger pathways by heteromeric G proteins [1,5]. In mammals, seven genes encode P2X subunits ($P2X_{1-7}$) that can form homo- and heterotrimeric cation channels with noticeable Ca^{2+} permeability [6,7]. Eight purinergic GPCRs ($P2Y_{1,2,4,6,11,12,13,14}$) have been identified and shown to exhibit distinctive specificities to nucleotides, depending on species [1,5]. For human isoforms, ATP serves as a full agonist for $P2Y_2$ and $P2Y_{11}$ but antagonizes $P2Y_4$, ADP is recognized by $P2Y_1$, $P2Y_{12}$, and $P2Y_{13}$, UTP is a full agonist for $P2Y_2$ and $P2Y_4$, UDP effectively stimulates $P2Y_6$ and $P2Y_{14}$ that also detects UDP-glucose and UDP-galactose. The $P2Y_{1,2,4,6,11}$ subtypes are canonically coupled by G_q/G_{11} to the phosphoinositide cascade and Ca^{2+} mobilization, whereas $P2Y_{12,13,14}$ control cAMP production by inhibiting adenylyl cyclase (AC) through G_i/G_o. In addition to G_q/G_{11}, $P2Y_2$ can couple to G_i, liberating βγ-complex that activates phospholipase beta, while the unique capability of $P2Y_{11}$

* Corresponding author at: Institute of Cell Biophysics, Russian Academy of Sciences, Institutional Street 3, Pushchino, Moscow Region, 142290, Russia.
E-mail address: staskolesnikov@yahoo.com (S.S. Kolesnikov).

https://doi.org/10.1016/j.ceca.2017.11.001
Received 19 July 2017; Received in revised form 25 October 2017; Accepted 6 November 2017
Available online 07 November 2017
0143-4160/

is to stimulate G_s [1]. P2Y agonists and antagonists are capable of eliciting a large variety of biological effects because apart from ubiquitous coupling to phospholipase C (PLC) and AC, P2Y receptors can also engage such effectors as MAP, PI3, Akt, and PKC kinases, small G-proteins, NO synthase, transactivation of growth factor receptors, and others [8–11].

Mesenchymal stromal cells (MSCs) are described as a heterogeneous cellular pool that includes immature cells responsible for the replenishment of supportive and connective tissues due to their capability to maintain self-renewal and multipotent differentiation [12–14]. The unique biologic properties of these cells attract sufficient interest in the fields of regenerative medicine and immunotherapy [15]. Damaged tissues are an abundant source of extracellular ATP that may be converted by extracellular nucleotidases to ADP and eventually to adenosine [3]. Meanwhile, purinergic agonists acting via multiple purinoreceptors have been documented as an important factor determining MSC fate [16–20]. In particular, ATP serves both as an adipogenic regulator and an osteogenic factor, while its downstream product adenosine switches off adipogenic differentiation and promotes osteogenesis [21,22]. Therefore, MSCs should be exposed to and regulated by nucleotides and adenosine when these cells migrate ***in vivo*** or are transplanted ***ex vivo*** into an injured tissue.

Among MSCs from different sources, adenosine receptors were identified first in human bone marrow-derived MSCs (BM-MSCs) by Evans and co-authors [23], which reported on expression of all four isoforms and posed adenosine as an important regulator of osteoclastogenesis and secretion of the inflammatory cytokine IL-6. Subsequent works implicated adenosine and A_{2B} receptors in regulating differentiation of human and mice BM-MSCs into osteoblasts or adipocytes [24–26]. To maintain spontaneous Ca^{2+} oscillations, BM-MSCs release ATP via hemichannels, providing autocrine stimulation of $P2Y_1$ receptors [27]. Reportedly, human adipose tissue-derived MSCs express most of the 15 P2 receptor subtypes, including, $P2X_3$-$P2X_7$ and all P2Y isoforms [28]. Although importance of P2X receptors for MSC physiology is largely undetermined, it has been speculated that $P2X_5$-$P2X_7$ are involved in osteogenesis [28–30] and migration [31]. Multiple studies implicate P2Y receptors in MSC proliferation ($P2Y_1$, $P2Y_{11}$), osteogenesis ($P2Y_2$, $P2Y_{13}$), and adipogenesis ($P2Y_1$, $P2Y_4$, $P2Y_{11}$, $P2Y_{14}$) [21,28,32–34].

Although growing evidence points at the purinergic signaling system as an essential part of a regulatory circuit that controls homeostasis and functionality of MSCs, coupling of P1 and P2 receptors to intracellular signaling pathways in these cells is detailed insufficiently. Being intrinsic to a MSC population [35,36], molecular and functional heterogeneity significantly complicates the analysis of intracellular signaling in MSCs at the level of individual cells. Here we employed the inhibitory analysis, Ca^{2+} imaging, and Ca^{2+} uncaging to examine Ca^{2+} signaling initiated by P2Y agonists in MSCs derived from the human adipose tissue. By using isoform-specific agonists and antagonists, we tried to identify P2Y subtypes coupled to Ca^{2+} mobilization in individual MSCs. While at the level of MSC population, we revealed expression of multiple P2Y isoforms, including $P2Y_1$, $P2Y_2$, $P2Y_4$, $P2Y_6$, $P2Y_{11}$, $P2Y_{13}$, and $P2Y_{14}$, MSC responsiveness to natural and synthetic P2Y agonists markedly varied from cell to cell. Perhaps, an individual MSC employs a specific set of P2Y receptors coupled to Ca^{2+} mobilization.

2. Materials and methods

2.1. Cell isolation and culturing

In this study, all procedures that involved human participants were performed in accordance with the ethical standards approved by the Bioethical Committee of Faculty of Basic Medicine at Lomonosov Moscow State University based on the 1964 Helsinki declaration and its later amendments. The study involved 15 healthy (not suffered from infectious or systemic diseases and malignancies) individuals from 21 to 55 years old, and informed consent was obtained from each participant.

MSCs were isolated from subcutaneous fat tissue of healthy donors of 21–55 years of age using enzymatic digestion as previously described [37]. Briefly, the adipose tissue was extensively washed with 2 volumes of Hank's Balanced Salt Solution (HBSS) containing 5% antibiotic/antimycotic solution (10,000 units of penicillin, 10,000 μg of streptomycin, and 25 μg of Amphotericin B per mL) (HyClone), fragmented, and then digested at 37 °C for 1 h in the presence of collagenase (200 U/ml, Sigma-Aldrich) and dispase (10 U/ml, BD Biosciences). Enzymatic activity was neutralized by adding an equal volume of culture medium (Advance Stem basal medium for human undifferentiated mesenchymal stem cells containing 10% of Advance stem cell growth supplement (CGS), 1% antibiotic/antimycotic solution (HyClone)) and centrifuged at 200 g for 10 min. This led to the sedimentation of diverse cells, including MSCs, macrophages, lymphocytes, and erythrocytes, unlike adipocytes that remained floating. After removal of supernatant, a lysis solution (154 mM NH_4Cl, 10 mM $KHCO_3$, and 0.1 mM EDTA) was added to a cell pellet to lyse erythrocytes, and cell suspension was centrifuged at 200 g for 10 min. Sedimented cells were re-suspended in the MSC culture medium and filtered through a 100 μm nylon cell strainer (BD Biosciences). As indicated by flow cytometry [38], after isolation and overnight pre-plating, the obtained cell population contained not only MSC cells that basically represented the most abundant subgroup but also admixed macrophages and lymphocytes. The two last cell subgroups were dramatically depleted by culturing for a week in the MSC culture medium and humidified atmosphere (5% CO_2) at 37 °C. The obtained MSC population was maintained at a sub-confluent level (~80% confluency) and passaged using HyQTase (HyClone). By using the methodology described previously [39], cultured cells were demonstrated to differentiate into the osteogenic, chondrogenic and adipogenic directions, the finding confirming their multipotency. In experiments, MSCs of the second to fourth passages were usually used.

2.2. RT-PCR

Total RNA was extracted from a sample containing 10^5-10^6 MSCs by using the RNeasy mini kit (Qiagen). Isolated RNA was treated with DNase I (Ambion) and reverse-transcribed with PrimeScript reverse transcriptase (Takara) and random hexamer primers, following manufacturer's instruction. Obtained cDNA served as a template for PCR with gene-specific primers that were designed to recognize all splice variants of human purinoreceptor genes and four genes encoding cell surface markers for MSCs, including CD73, CD90, CD105, and MCAM (Table 1).

2.3. Preparation of cells for Ca^{2+} imaging

Before assaying with Ca^{2+} imaging, cells were maintained in a 12-socket plate for 12 h in the medium described above but without antibiotics. For isolation, cells cultured in a 1 ml socket were rinsed twice with the Versen solution (Sigma-Aldrich) that was then substituted for 200 μl HyQTase solution (HyClone) for 3–5 min. The enzymatic treatment was terminated by the addition of a 0.8 ml culture medium to a socket. Next, cells were re-suspended, put into a tube, and centrifuged at 50 g for 45 s for sedimentation. Isolated cells were collected by a plastic pipette and plated onto a photometric chamber of nearly 150 μl volume. The last was a disposable coverslip (Menzel-Glaser) with attached ellipsoidal resin wall. The chamber bottom was coated with Cell-Tak (BD Biosciences), enabling strong cell adhesion. Attached cells were then loaded with dyes for 20 min at room temperature (23–25°Ñ) by adding Fluo-4AM (4 μM) or Fluo-4AM (4 μM) + NP-EGTA-AM (4 μM) and Pluronic (0.02%) (all from Molecular Probes) to a bath solution. Loaded cells were rinsed with the bath solution for several times. and kept at 4 °C for 1 hour prior to recordings. Generally, incubation of MSCs at low temperature stabilized intracellular Ca^{2+} and

Table 1
Sequences of gene-specific primers.

Subgroup	Target gene	5′-sequence-3′ (Forward/Reversed)	Product size (bp)
P1 receptors	A1	TCCATCTCAGCTTTCCAGG TCACCACCATCTTGTACCG	349
	A2A	CAGAACGTCACCAACTACTTTG GGTCACCAAGCCATTGTACC	240
	A2B	ATGCTGCTGGAGACACAGG CCGTGACCAAACTTTTATACCT	355
	A3	AGAGATCACCCCACCAGAAAAG GAGTGGTGACCCTCTTGTATC	537
P2Y receptors	P2Y1	TTCTTGGCGGGAGATACTTTC ACAAGCTAAGTGTGGATGTGG	319
	P2Y2	ACCTGATTAGAGTGTGCAACG TCTAACAGTTTAATTCCACGCCAG	387
	P2Y4	ACAAATATCGACGTCAGCTCCG CTGGAAAAGAGGAAGAAGCACC	268
	P2Y6	AGTCCAAGGAGTCAGGAAAGAG TTGTCTGGAGGGTAGCTGAAG	258
	P2Y11	CACCCTCTACTCTACATGGC CTCCACTCTCTCTACTTGGTTC	466
	P2Y12	CCTAGTCCCCTAACCAAATCC CAGTAGTTATGCTGTGCAACTTTG	458
	P2Y13	ACGTTTTCTTCCATGGCCTC GGTGATTGGGTTTGAGGTG	270
	P2Y14	CCTGGGGTTCTGGTGTTAG GTCAGTAACCGTATGCCATGTC	331
P2X receptors	P2X1	CACGCTTCAAGGTCAACAGG CACAAAGTGCCTGGCAAACC	308
	P2X2	CCCAAATTCCACTTCTCCAAG TCTTGTAGTATTTGGCAAACCTG	310
	P2X3	CAGGCTACAACTTCAGGTTTG AGCGTAGTCTCATTCACCTC	271
	P2X4	CCCAAATTTAATTTCAGCAAGAG GATGATGTCAAATTTCCCTGC	414
	P2X5	CAAGAAGTACGAGGAAGTGAGG AGGCAATTCACGTGCTCCTG	233
	P2X6	CACACACAGCCACGGTGTAA ATGCCTACAGAGCCACCCA	348
	P2X7	CTCTCCTACTTCGGTCTGG TGAAGTCCATCGCAGGTCTT	299
Cell surface markers	CD73	AAGACATGACTCTGGTGACC CTGTCACAAAGCCAGGTCC	266
	CD90	GTCACAGTGCTCAGAGAC TACAAAAAGACAGCCAGAGG	344
	CD105	AGCAGAGCTTTGTGCAGGTC GCTGATGATGTTCAAGCGCATG	317
	MCAM	AGGGAAGCAGGAGATCACG GGCTTCTCTCTAGTCCCTTTG	266

decreased a fraction of spontaneously oscillating cells.

2.4. Ca^{2+} imaging and uncaging

Experiments were carried out using an inverted fluorescent microscope Axiovert 135 equipped with an objective Plan NeoFluar 20x/0.75 (Zeiss) and a digital ECCD camera LucaR (Andor Technology). Apart from a transparent light illuminator, the microscope was equipped with a hand-made system for epi-illumination via an objective. The epi-illumination was performed using a bifurcational glass fiber. One channel was used for Fluo-4 excitation and transmitted irradiation of a computer-controllable light-emitting diode (LED) LZ1-00B700H (Ledengin). LED emission was filtered with an optical filter ET480/20 x (Chroma Technology). Fluo-4 emission was collected at 535 ± 25 nm by using an emission filter ET535/50m (Chroma Technology). Serial fluorescent images were usually captured every second and analyzed using Imaging Workbench 6 software (INDEC). Deviations of cytosolic Ca^{2+} from the resting level were quantified by a relative change in the intensity of Fluo-4 fluorescence ($\Delta F/F_0$) recorded from an individual cell. Another channel was connected to a pulsed solid laser TECH-351 Advanced (680 mW) (Laser-Export, Moscow). This unit operated in a two-harmonic mode and generated not only 351 nM UV light used for Ca^{2+} uncaging but also visible light at 527 nm. The last could penetrate into an emission channel through non-ideal optical filters and elicit optical artifacts during uncaging. For Ca^{2+} uncaging, cells were loaded with both 4 μM Fluo-4 and NP-EGTA (both from Invitrogen). In certain cases, cells that were initially loaded with Fluo-4 alone were additionally stained in the presence of 4 μM NP-EGTA-AM + 0.02% Pluronic during recordings. The basic bath solution contained (mM): 110 NaCl, 5.5 KCl, 2 $CaCl_2$, 0.8 $MgSO_4$, 10 glucose, 10 HEPES-NaOH, pH 7.4 (~270 Osm). When necessary, 2 mM $CaCl_2$ in the bath was replaced with 0.5 mM EGTA + 0.4 mM $CaCl_2$, thus reducing free Ca^{2+} to nearly 260 nM at 23 °C as calculated with the Maxchelator program (http://maxchelator.stanford.edu). In this low Ca^{2+} bath solution, the glucose concentration was increased to 13 mM to keep osmolarity. All chemicals used in experiments described below were applied by the complete replacement of the bath solution in a 150 μl photometric chamber for nearly 2 s using a perfusion system driven by gravity. The used salts and buffers were from Sigma-Aldrich, agonists and inhibitors were from Tocris.

2.5. Immunostaining

Cultured cells were first washed with PBS and fixed in 4% formaldehyde for 4 min at room temperature. Cells were then washed with PBS. The nonspecific binding was blocked by incubation in 1% BSA with 10% normal goat serum for 30 min. Immunostaining was performed using rabbit antibody against $P2Y_{11}$ receptor (Alomone labs). Cells stained with primary antibody were rinsed and incubated with goat anti-rabbit IgG conjugated with AlexaFluor 594 (Invitrogen). Cells were counterstained with the nuclear dye DAPI (4,6-diamidino-2-phenylindole, Molecular Probes). As a negative control, cells were incubated with rabbit nonspecific IgG instead of the primary antibody. Immunofluorescence was analyzed using a Leica DMI6000 B microscope equipped with a Leica DFC7000T camera and Las X software (Leica).

3. Results

In a typical experiment, 120-180 MSCs loaded with Fluo-4 resided in a photometric camera, and their fluorescent images were captured every second. During Ca^{2+} imaging acquisition 480-nm LED was switched-on for only 200 ms per period, thereby minimizing photobleaching of Fluo-4 at a sufficiently high signal-to-noise ratio that was achieved by adjusting LED emission. This acquisition protocol enabled us to reliably assay cell responsiveness to different compounds for up to 60 min. In a particular MSC sample, ATP and other P2Y agonists stimulated Ca^{2+} signaling in a 7-15% fraction of cells. Here we called such MSCs purinergic, although cells found nonresponsive, in terms of Ca^{2+} signaling, also might be purinergic in that P2Y agonists could stimulate diverse signaling events in their cytoplasm, which were undetectable with Ca^{2+} imaging.

In our hands, MSCs were mostly sensitive to ATP, ADP, and UTP. Particularly, the short application of 3 μM ATP, 3 μM ADP, or 10 μM UTP triggered marked Ca^{2+} transients, frequently of the oscillatory character, depending on stimulus duration (Fig. 1A, cell 1). It appeared that responsiveness to ATP, ADP, and UTP was more or less universal for MSC populations obtained from different donors. In contrast, the vast majority of purinergic MSCs were insensitive to UDP applied at 10–50 μM (Fig. 1A). Specifically, among MSC preparations that were obtained from adipose tissues of 15 individuals, only 2 donors provided a cellular material that contained UDP-responsive MSCs. In these rare MSC colonies, we identified 127 purinergic cells overall, and among them, 15 cells (12%) reacted to 10 μM UDP (see below) by generating ADP-like responses (Fig. 1A, cells 1 and 2).

In a number of special experiments, we examined MSC responsivity to the particular nucleotide by stimulating cells with ATP, ADP, and

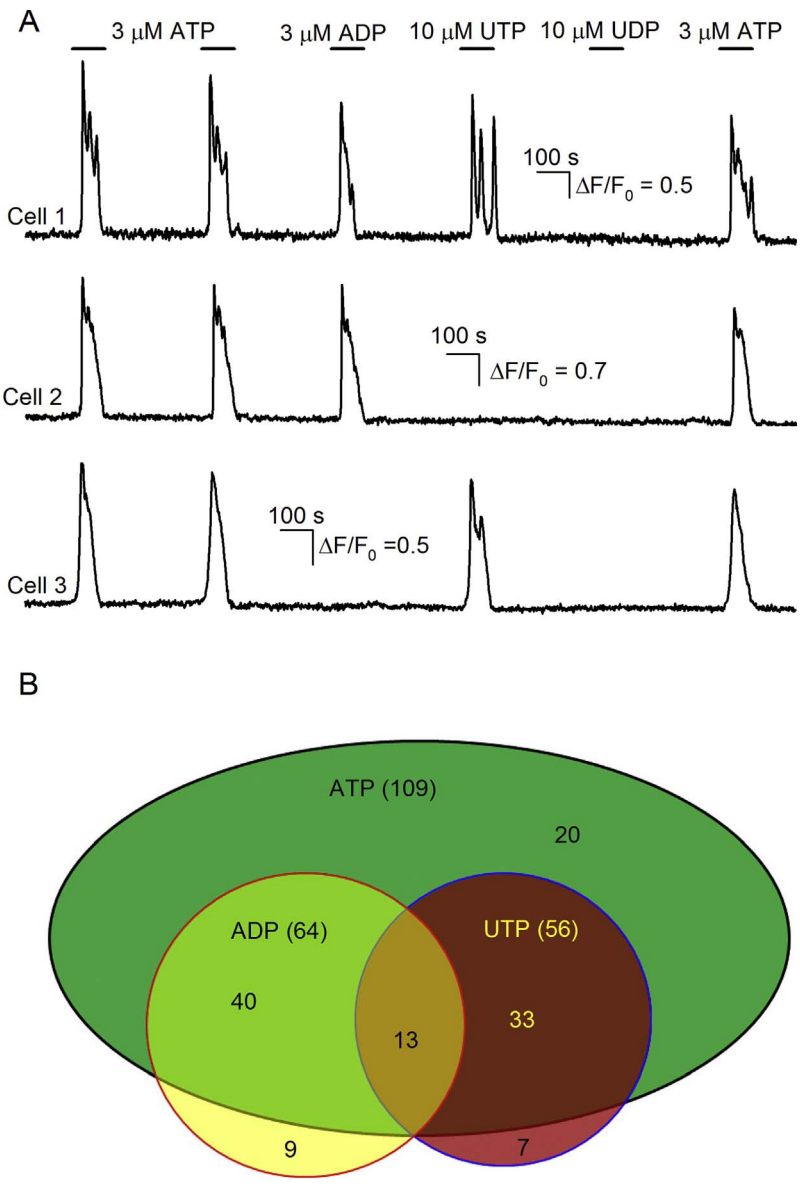

Fig. 1. Responsiveness of MSCs to natural purinergic agonists. (*A*) Representative concurrent recordings from 3 individual MSCs stimulated with 3 μM ATP, 3 μM ADP, 10 μM UTP, and 10 μM UDP. The indicated nucleotide doses were 2-3 times higher than the threshold concentration characteristic of the particular agonist. Here and in the below figures: applications of compounds are indicated by the straight-line segments above the experimental trace (Cell 1); the data are presented as $\Delta F/F_0$, where $\Delta F = F\text{-}F_0$, F is the instant intensity of cell fluorescence, F_0 is the intensity of cell fluorescence obtained in the very beginning of a recording and averaged over a 20-s interval. (*B*) Venn diagram for the distribution of cell responsivity to 3 μM ATP, 3 μM ADP, and 10 μM UTP among 125 purinergic MSCs.

UTP that were applied sequentially. Among 125 MSCs assayed overall, we found only 13 cells (10%) to be responsive to all three agonists at the indicated concentrations (Fig. 1A). Both ATP and ADP stimulated Ca^{2+} signaling in 40 cells (32%) that did not respond to UTP; 33 cells (26%) preferred the ATP-UTP pair. In addition, 20, 9, and 7 cells (16, 7, and 6%) responded exclusively to ATP, ADP, or UTP, respectively (Fig. 1B). The abovementioned findings suggest that: (i) functional expression of particular P2Y receptors and/or their coupling to Ca^{2+} mobilization varied from cell to cell; (ii) P2X receptors play a minor, if any, role in mediating MSC responses to ATP, given that by kinetics and magnitude, ATP-sensitive cells generated basically similar Ca^{2+} transients on ADP or UTP (Fig. 1A).

3.1. Expression of P1 and P2 receptors in MSCs

We searched for transcripts for all known purinoreceptors in MSC populations by using conventional RT-PCR and specific primers that were designed based on available sequences of human genes encoding four adenosine receptors (A_1, A_{2A}, A_{2B}, and A_3) [4], eight P2Y receptors ($P2Y_{1,2,4,6,11\text{-}14}$), and seven P2X receptors ($P2X_{1\text{-}7}$) [40,41] (Materials and Methods, Table 1). Template RNA was isolated from MSC samples ($\sim 10^6$ cells) that were derived from adipose tissues of 7 individuals. In 5 different donor-related MSC colonies, UDP-responsive cells were not found, while 2 MSC colonies contained such cells. In all RNA samples, we detected basically the same set of transcripts for purinoreceptors as well as for cell surface markers for MSCs (CD73, CD90, CD105, and MCAM) (Fig. 2). In particular, we identified transcripts for A_1, A_{2A}, and A_{2B} receptors, albeit no evidence for expression of the A_3 receptor was obtained (Fig. 2A). Transcripts for $P2Y_1$, $P2Y_2$, $P2Y_4$, $P2Y_6$, $P2Y_{11}$, $P2Y_{13}$ and $P2Y_{14}$ receptors were revealed, while $P2Y_{12}$ transcripts were not detected (Fig. 2B). Besides, we obtained amplicons related to $P2X_2$, $P2X_4$, and $P2X_7$ receptors but failed to detect transcripts for $P2X_1$, $P2X_3$, $P2X_5$, and $P2X_6$ receptors (Fig. 2C). The array of P2Y receptors identified by us in MSCs is rather sufficient to account for their responsiveness to ATP, ADP, and UTP (Fig. 1). It was however surprising that all MSC samples contained transcripts for the UDP receptors $P2Y_6$ and $P2Y_{14}$, although UDP-responsive cells were identified only in 2 of them (see below).

3.2. Dose-response dependence

Similar to adrenergic MSCs [38], purinergic cells responded to agonists in an “all-or-nothing” manner. Specifically, ATP and other nucleotides either exerted undetectable effects or initiated quite similar

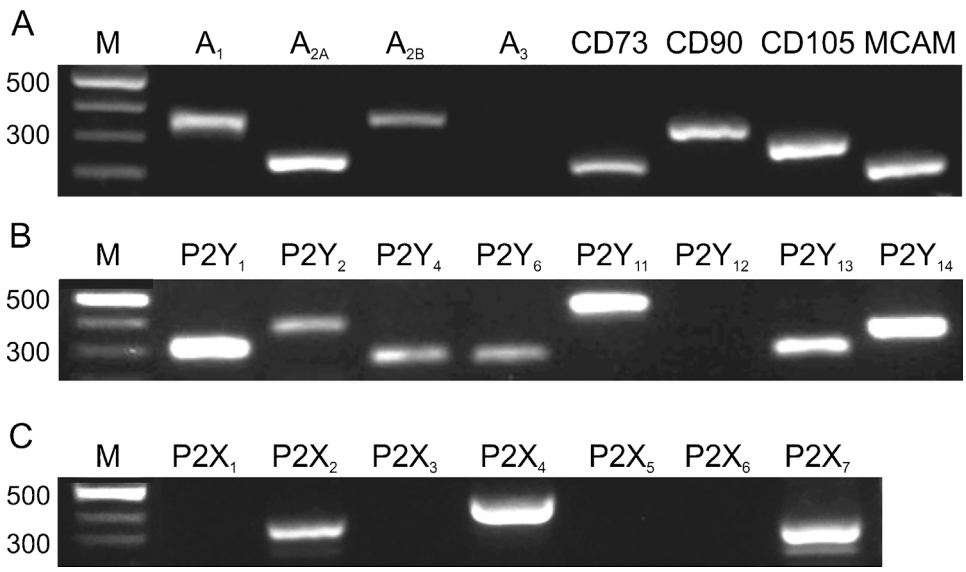

Fig. 2. Detection of purinoreceptor transcripts expressed in MSCs. (*A*) Representative set (n = 7) of transcripts for human P1 receptors and cell surface marker proteins. The detected transcripts of the expected sizes of 349, 240, and 355 bp correspond to the A_1, A_{2A}, A_{2B} receptors, respectively. Each RNA sample also contained transcripts for CD73 (266 bp), CD90 (344 bp), CD105 (317 bp), and MCAM (266 bp) that are conventionally considered as cell surface markers of undifferentiated MSCs. Transcripts for the A_3 receptor (537 bp) were undetectable. The molecular weight markers (M) were from GeneRuler 100 bp DNA Ladder (Fermentas). (*B*) Representative set of P2Y transcripts detected in MSC preparations (n = 7). The products of expected sizes were amplified for $P2Y_1$ (319 bp), $P2Y_2$ (387 bp), $P2Y_4$ (268 bp), $P2Y_6$ (258 bp), $P2Y_{11}$ (466 bp), $P2Y_{13}$ (270 bp), and $P2Y_{14}$ (331 bp) but not for $P2Y_{12}$ (458 bp). (*C*) Detection of P2X transcripts in MSC preparations (n = 7). The products of expected sizes were amplified for $P2X_2$ (310 bp), $P2X_4$ (414 bp), and $P2X_7$ (299 bp) but not for $P2X_1$ (308 bp), $P2X_3$ (271 bp), $P2X_5$ (233 bp), and $P2X_6$ (348 bp).

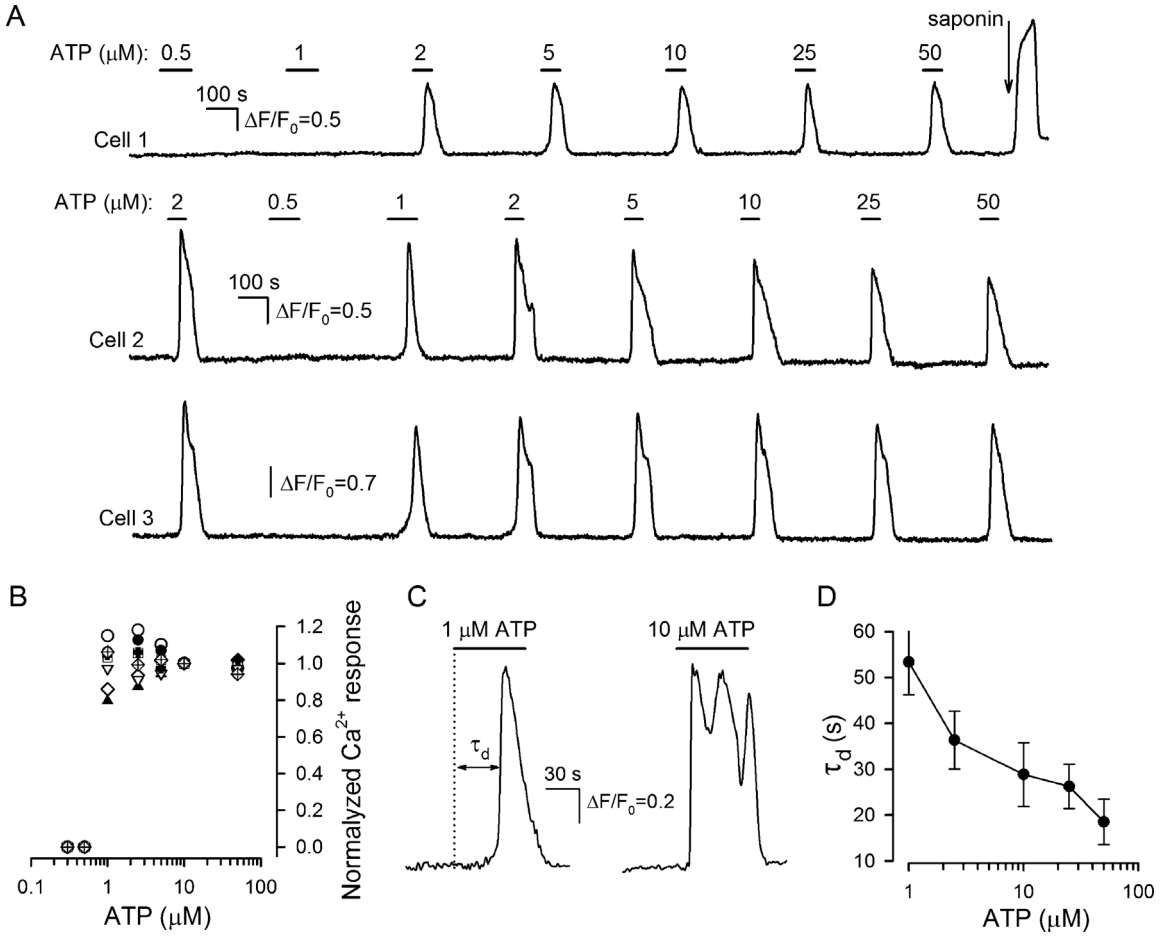

Fig. 3. Dose dependence of ATP responses. (*A*) Monitoring of intracellular Ca^{2+} in three different MSCs serially stimulated by ATP at variable concentrations as indicated. Cell 1, in the end of the recording, 0.1 mg/ml saponin was applied (arrow) to demonstrate that Fluo-4 fluorescence was not saturated by Ca^{2+} bursts elicited by ATP. The saponin-induced Ca^{2+} transient spontaneously declined presumably due to Fluo-4 leakage via saponin pores. Cells 2 and 3 were assayed simultaneously. (*B*) Superimposed dose dependences of ATP responses recorded from 8 cells that exhibited the threshold of 1 μM. In each case, ATP responses were normalized to a response elicited by 10 μM ATP. Each symbol corresponds to an individual cell. (*C*) Representative Ca^{2+} transients elicited by ATP at 1 μM (threshold concentration) and 10 μM in the same cell. These ATP responses were delayed relative to the moment of agonist application by 43 s and 22 s, respectively. The characteristic time of the response delay (τ_d) was calculated as a time interval necessary for a Ca^{2+} transient to reach the half-magnitude value (left panel). (*D*) Dependence of a response lag on ATP concentration. The data obtained from 8 different cells are presented as a mean ± S.D.

Ca^{2+} responses at different doses above the threshold value. As a rule, submicromolar ATP was ineffective, while at 1–2 μM and higher, the nucleotide stimulated Ca^{2+} transients in the MSC cytoplasm (Fig. 3A). For ADP- and UTP-responses, the threshold concentrations ranged within 0.5–2 μM and 3–6 μM, respectively. Among purinergic MSCs, certain cells, presumably most robust, remained responsive for up to 40–60 min, allowing for the analysis of their sensitivity to ATP in a wide range of concentrations varied within 0.5–50 μM. During this prolonged assay responsiveness of many cells was liable to rundown, thus hampering quantitative analysis. Nevertheless in this series, we identified 32 cells that allowed for conclusive recordings. Among them, 9 MSCs generated quite similar Ca^{2+} signals at gradually increasing ATP doses (Fig. 3A, cell 1). We considered the possibility that these cellular responses seemed alike because ATP elicited too high Ca^{2+} transients, which all saturated Fluo-4 fluorescence and therefore could not be discriminated by magnitude. However, when MSCs were treated with the permeabilizing agent saponin (0.1 mg/mL), it caused marked Ca^{2+} signals that exceeded ATP responses by a factor of 1.5-2 (17 cells) (Fig. 3A, cell 1). These observations indicated conclusively that cellular responses to ATP or to other nucleotides could not be equalized by the saturation of the Ca^{2+} dye.

ATP responses were liable to some rundown in 16 cells assayed in this series (Fig. 3A, cell 2). Seven cells exhibited large (> 75%) but not maximal responses at the threshold stimulation and generated Ca^{2+} transients slightly increasing with ATP dose (Fig. 3A, cell 3). In any event, none of the cells generated serial Ca^{2+} responses that would gradually vary by value from poorly detectable to saturating one when bath ATP was increased from 0.5 to 50 μM. Note that before a whole-range assay, a MSC population was typically stimulated with 2–3 μM ATP to identify purinergic cells and to exclude others from subsequent photometric acquisition. This very first stimulation elicited a somewhat higher Ca^{2+} transient in a cell compared to posterior ATP responses (Fig. 3A). Perhaps, the initial ATP application stimulated a long-lasting feedback process that regulated MSC responsiveness to the nucleotide.

For quantitative analysis, we took 8 MSCs that robustly responded to varied ATP at the same threshold of 1 μM. As summarized in Fig. 3B, each individual cell demonstrated a step-like dose-response curve. Whereas assayed cells generated biphasic responses to ATP at the threshold concentration (Fig. 3C, left panel), oscillatory responses could occur at 10 μM ATP and higher, depending on stimulus duration (Fig. 3C, right panel). In all cases, an ATP response was markedly deferred relative to the moment of nucleotide application (Fig. 3C), and the response delay monotonically shortened as ATP concentration increased. For cells responsive to 1 μM ATP, Ca^{2+} transients were retarded by 41–65 s at the threshold stimulation, and the lag reduced to 11–27 s at 50 μM ATP (Fig. 3D). Although we did not characterized MSC responses to ADP and UTP at widely varied concentrations, it could be expected that dose-response and dose-delay curves for both agonists would be similar to those obtained for ATP (Fig. 3B-D). Indeed, Ca^{2+} transients of close magnitudes were usually elicited by ADP at 1 and 30 μM but responses to 1 μM ADP were nearly twice more delayed compared to responses elicited by 30 μM ADP (16 cells). Cellular responses to UTP altered similarly when the agonist dose was increased from 3 μM to 50 μM (11 cells) (Supplementary Materials, Fig. 1S).

It is noteworthy that in contrast to our findings (Fig. 3A, B), a gradual dose-dependence of ATP responses was demonstrated in the recent study of MSCs derived from human dental pulp (hDP-MSCs) [31]. This discrepancy can be explained by that ATP responsiveness of hDP-MSC was assayed at the populational level, and the authors did not study individual cells. Being averaged over a population, a step-like dose-dependence should be smoothed because individual cells differently accumulate Ca^{2+} dyes and generate Ca^{2+} bursts on agonists with dissimilar threshold, lag, kinetics, and magnitude.

3.3. Purinergic transduction involves the phosphoinositide cascade and Ca^{2+}-induced Ca^{2+} release

In further experiments, we analyzed coupling of P2Y receptors to Ca^{2+} mobilization in the MSC cytoplasm. When purinergic MSCs were pretreated with U73122 (2 μM), a poorly reversible inhibitor of PLC, all assayed cells became completely nonresponsive to ATP (39 cells) (Fig. 4A, D) as well as to UTP (7 cells) and ADP (5 cells) (Fig. 2S). The effects of U73122 were specific as the much less effective analog U73343 (2 μM) never canceled MSC responses to the nucleotides (Fig. 4A, D) (39 cells). Moreover, the decrease of bath Ca^{2+} from 2 mM to 260 nM weakly or negligibly affected Ca^{2+} transients in the MSC cytoplasm elicited by ATP (26 cells) (Fig. 4B, D) as well as by UTP (14 cells) and ADP (13 cells) (Fig. 2S). Thus, these nucleotides stimulated Ca^{2+} signaling in MSCs by involving purinoreceptors that were coupled by the phosphoinositide cascade basically to Ca^{2+} release rather than to Ca^{2+} entry. Together, these findings indicated that P2X receptors could provide only a weak, if any, contribution to Ca^{2+} signals elicited by ATP in the MSC cytoplasm (Figs. 1 A, 3 A).

Being a common effector downstream of PLC [42], the IP_3 receptor should have been involved in coupling of P2Y receptors to Ca^{2+} mobilization in MSCs. As expected, the IP_3 receptor blocker 2-APB (50 μM) suppressed ATP responses, while 50 μM ryanodine, a ryanodine receptor antagonist, was ineffective (Fig. 4C, D) (21 cells). These findings suggested a negligible role for ryanodine receptors in ATP transduction. Consistently, their agonist caffeine (10 mM) insignificantly affected cytosolic Ca^{2+} in purinergic MSCs (7 cells) (Fig. 4C). Similar to ATP responses, 50 μM 2-APB rendered MSCs insensitive to 3 μM ADP and 10 μM UTP as well (4 and 5 cells, respectively) (Fig. 2S). Note that 2-APB blocks not only IP_3 receptors but also a variety of Ca^{2+}-entry channels [43–45]. Given however that MSC responsiveness to P2Y agonists insignificantly depended on bath Ca^{2+} and therefore on Ca^{2+} influx (Fig. 4B, D), we inferred that 2-APB exerted the inhibitory action (Fig. 4C) largely by targeting IP_3 receptors.

Our previous analysis of MSC responsivity to adrenergic agonists implicated Ca^{2+}-induced Ca^{2+} release (CICR) in mediating cellular responses [38]. Being ubiquitously involved in intracellular Ca^{2+} signaling, CICR might contribute to purinergic transduction as well, and the dose-dependence of ATP responses indirectly supported this idea (Fig. 3A, B). Indeed, to generate ATP responses in an “all-or-nothing” manner, MSCs should have employed a specialized mechanism for equalizing Ca^{2+} transients elicited by ATP at different doses. The trigger-like CICR mechanism appeared to be an appropriate candidate. The functionality of CICR in purinergic MSCs was validated with Ca^{2+} uncaging that allowed one to generate as fast and intensive cytosolic Ca^{2+} bursts as necessary for initiating the CICR process. In designed experiments, MSCs were preloaded with both Fluo-4 and photolabile Ca^{2+} chelator NP-EGTA; sometimes Fluo-4 loaded cells were additionally stained with NP-EGTA during assaying. Because a UV laser we employed for uncaging was in fact a biharmonic light source emitting at 351 and 527 nm, a light stimulus caused an optical artifact that was seen as a marked overshoot in a recording trace of cell fluorescence acquired at 535 ± 25 nm.

In this series, we identified 37 purinergic MSCs, 24 of which (~65%) responded to UV pulses with biphasic Ca^{2+} transients that were similar to ATP-responses kinetically and by magnitude (Fig. 5A, D). In remaining 13 ATP-responsive cells (35%), Ca^{2+} uncaging elicited much smaller, exponentially relaxing Ca^{2+} signals as was the case with the third response in the recording depicted in Fig. 5C. In such MSCs, NP-EGTA loading might be insufficient and/or an IP_3 level might be too low at rest so that Ca^{2+} uncaging failed to trigger CICR. Interestingly, U73122 weakly or negligibly affected Ca^{2+} transients elicited by UV flashes, although this PLC inhibitor rendered MSCs nonresponsive to ATP (n = 7) (Fig. 5B, D). This finding argued against the possibility that Ca^{2+} uncaging might initiate cellular response by stimulating Ca^{2+}-activated PLC isoforms [46], which quickly generated a sufficient

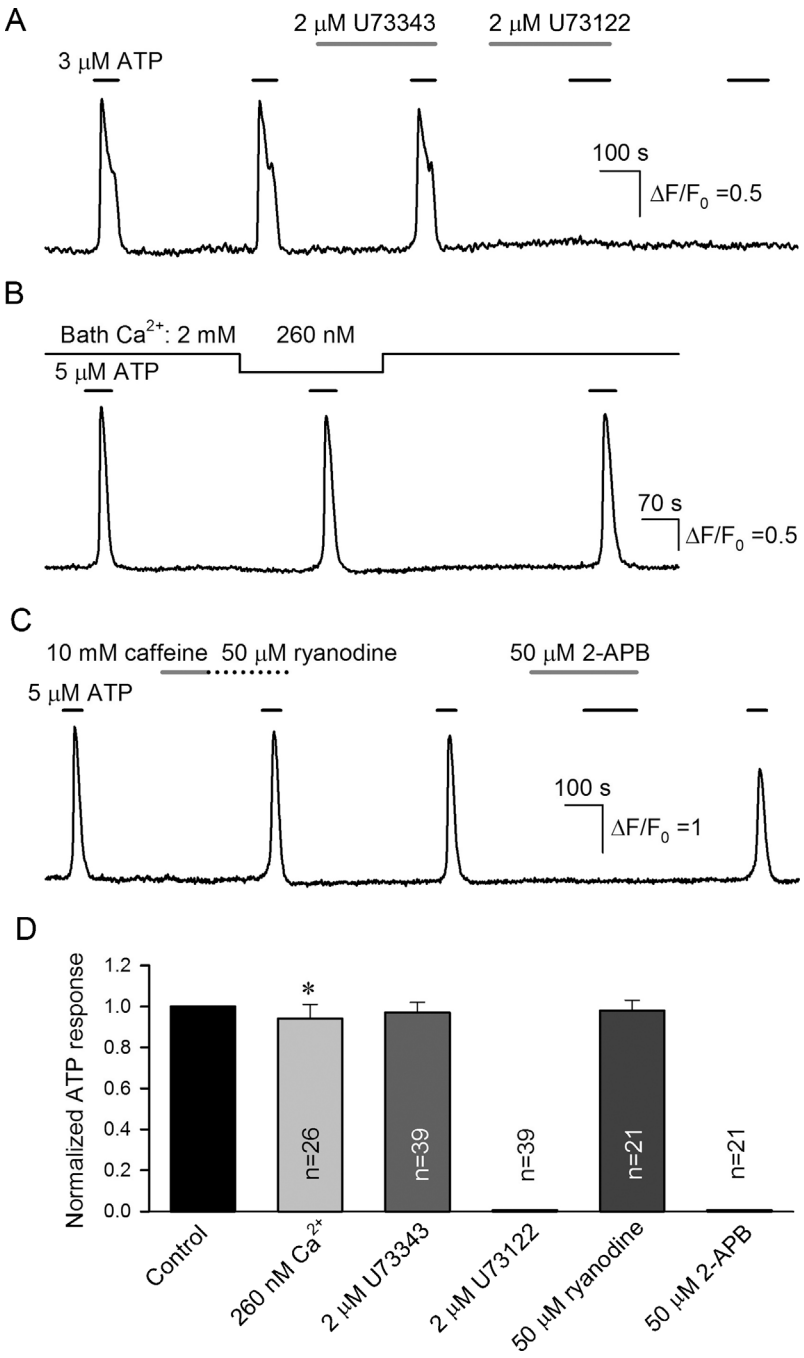

Fig. 4. Involvement of the phosphoinositide cascade in purinergic transduction. (*A*) PLC inhibitor U73122 (2 μM) irreversibly suppressed MSC responsivity to 3 μM ATP while the much less effective analog U73343 (2 μM) was ineffective. (*B*) Reduction of bath Ca^{2+} from 2 mM to 260 nM weakly or negligibly affected MSC responsivity to 5 μM ATP. Extracellular Ca^{2+} was not completely removed because usually, MSCs poorly tolerated prolonged exposure to a Ca^{2+}-free solution. (*C*) Unlike ryanodine, an antagonist of ryanodine receptors, the IP_3 receptor blocker 2-APB (50 μM) reversibly suppressed ATP responses. In (*A-C*), 3 different cells were assayed. (*D*) Summary of MSC responses to ATP (3–5 μM) in control and in the presence of different compounds. To compare different experiments, ATP responses in control were taken to equal 1. Given rundown of cell responsivity, the control ATP response was calculated as a half sum of the first and third ATP responses recorded during sequential application of ATP, low Ca^{2+}/ryanodine, and ATP. In all cases, ***n*** is the number of cells assayed under particular conditions. Asterisks indicate significant difference (Student t-test at $p < 0.05$).

IP_3 burst, thereby enhancing activity of IP_3 receptors and triggering CICR. However, the ineffectiveness of U73122 (Fig. 5B, D) indicated that PLC activation was not obligatory for generating light responses, strongly arguing that CICR initiated by UV-flashes was directly stimulated by Ca^{2+} ions liberated from NP-EGTA.

To evaluate a relative contribution of IP_3- and ryanodine receptors to CICR, we studied effects of their antagonists on Ca^{2+} signals associated with Ca^{2+} uncaging. While 50 μM ryanodine was ineffective (11 cells) (Fig. 5C, D), 50 μM 2-APB dramatically and reversibly changed a shape and magnitude of UV responses in purinergic MSCs (n = 11) (Fig. 5C, D). In control (Fig. 5A, 1st response; Fig. 5B, 3rd response) and in the presence of 50 μM ryanodine (Fig. 5C, 2nd response), Ca^{2+} uncaging elicited biphasic Ca^{2+} transients that were delayed relative to stimulatory UV flashes. Thus, despite the presence of ryanodine, Ca^{2+} uncaging was still capable of stimulating robust CICR in purinergic cells. With 50 μM 2-APB in the bath, a UV pulse entailed a brief Ca^{2+} jump that relaxed monotonically (Fig. 5C, 3nd response). This indicated that Ca^{2+} uncaging was unable to initiate CICR if IP_3 receptors were inhibited. Meanwhile, when 2-APB was removed to restore activity of IP_3 receptors, a UV flash triggered a biphasic Ca^{2+} transient again (Fig. 5C, 4th response). These observations indicated that just IP_3 receptors were basically responsible for CICR in purinergic cells.

3.4. Effects of isoform specific agonists and antsgonists of P2Yreceptors

Although the RT-PCR analysis revealed transcripts for $P2Y_1$, $P2Y_2$, $P2Y_4$, $P2Y_6$, $P2Y_{11}$, $P2Y_{13}$, and $P2Y_{14}$ in total MSC preparations (Fig. 2), it remained unclear whether a given cell utilized all identified P2Y receptors or a certain combination of them. The last possibility appeared to be more plausible because MSC responsiveness to natural P2Y agonists varied from cell to cell (Fig. 1). To assess a contribution of a particular P2Y receptor to responsiveness of individual MSCs, we used a

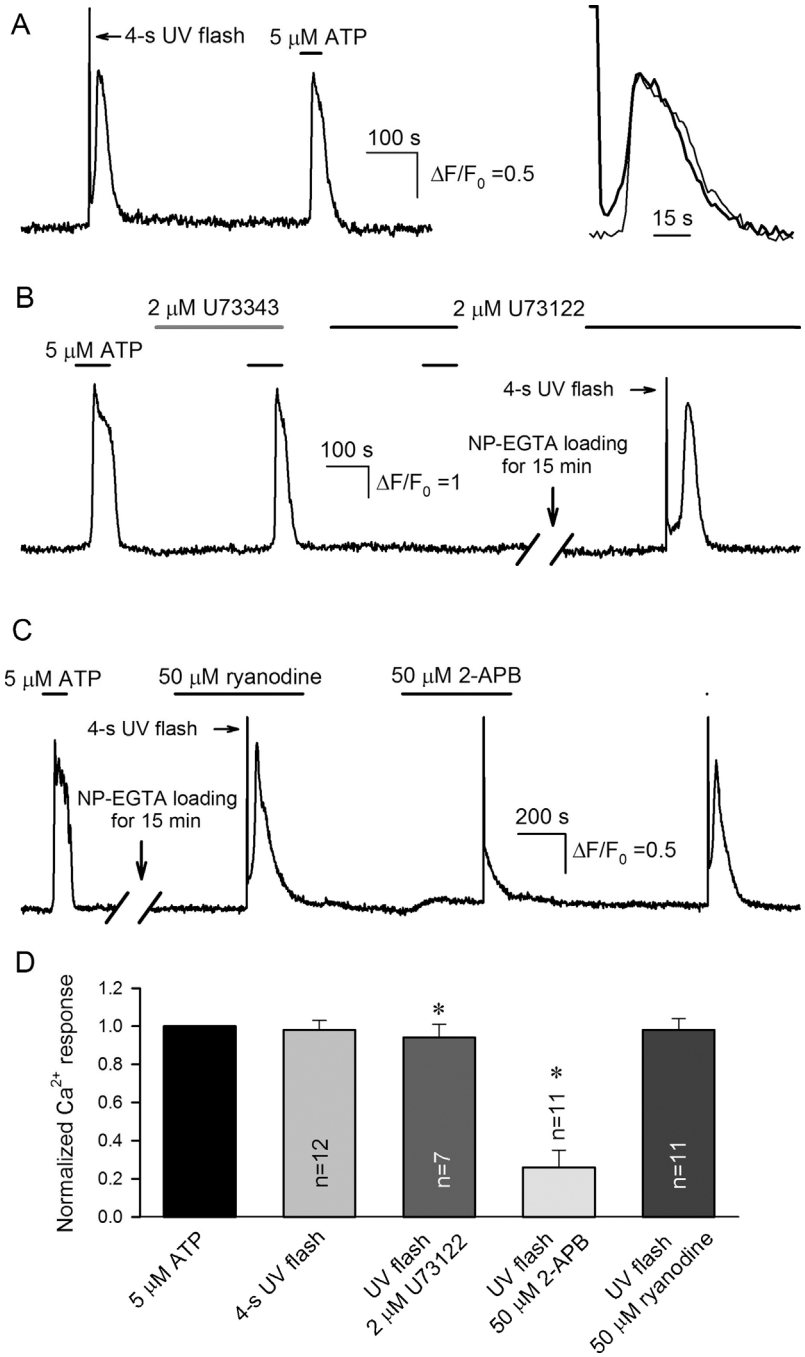

Fig. 5. Evidence for Ca^{2+}-induced Ca^{2+} release in purinergic MSCs. (*A*) Left panel, cellular responses to Ca^{2+} uncaging produced by a 4-s UV flash and to 5 μM ATP. The light and ATP responses shown in the left panel are superimposed in the right panel. (*B*) PLC inhibitor U73122 dumped MSC responsiveness to 5 μM ATP but did not prevent ATP response-like Ca^{2+} transients produced by Ca^{2+} uncaging. (*C*) In contrast to 50 μM ryanodine, 2-APB (50 μM) completely abolished biphasic ATP-like responses elicited by UV flashes. In all cases, cells were loaded with both Fluo-4 and NP-EGTA. In the presented experiments, emission of a UV laser was weakened by the factor ten, so that Ca^{2+} uncaging should have lasted for 4 s to liberate as many Ca^{2+} ions as necessary for stimulating CICR. This gradual release of caged Ca^{2+} somewhat slowed the rising phase of a biphasic Ca^{2+} transient produced by CICR, thereby making a lag between a UV flash and a light response clearly visible. (*D*) Summary of MSC responses to 5 μM ATP and Ca^{2+} uncaging under different conditions. To compare different experiments, Ca^{2+} responses elicited by UV flashes were normalized to an ATP response just preceding Ca^{2+} uncaging. Asterisks indicate significant difference (Student t-test at $p < 0.05$).

wide array of isoform-specific P2Y agonists and antagonists.

The human P2Y family contains two ATP receptors, including specialized $P2Y_{11}$ and also $P2Y_2$ that recognizes both UTP and ATP as full equipotent agonists [1]. Serving also as a partial $P2Y_1$ agonist of much lower affinity than ADP [47], ATP was hardly capable of stimulating $P2Y_1$-signaling in MSCs at low micromolar concentrations. We tried to evaluate a contribution of $P2Y_{11}$ and $P2Y_2$ to MSC responsiveness to ATP. Among 181 MSCs assayed in this series, 169 cells (93%) became nonresponsive to ATP (3 μM) in the presence of 30 μM NF 340, a specific $P2Y_{11}$ antagonist. These NF 340-sensitive cells did not respond to the $P2Y_2$ agonist MRS 2768 (10 μM) (Fig. 6A, cell 1). In a subpopulation of rare MSCs (12 cells) that were capable of generating Ca^{2+} transients on 3 μM ATP in the presence of NF 340, 11 cells also responded to 10 μM MRS 2768 (Fig. 6A, cell 2; Fig. 6B). Thus, these NF 340-insensitive cells presumably detected bath ATP by using $P2Y_2$ or both $P2Y_2$ and $P2Y_{11}$.

While the $P2Y_{11}$ antagonist was highly effective (Fig. 6A, B), most ATP-sensitive MSCs were surprisingly nonresponsive to NF 546 (10 μM), the $P2Y_{11}$ agonist that reportedly exceeds ATP by efficacy [48]. To address this inconsistency, we examined MSC responsivity to NAD^+ (nicotinamide adenine dinucleotide) and $NAADP^+$ (nicotinic acid adenine dinucleotide phosphate), the natural $P2Y_{11}$ agonists that enable coupling of this purinoreceptor to diverse intracellular pathways, including Ca^{2+} mobilization [49,50]. Note that in pilot experiments, we assayed 23 ATP-responsive MSCs and found that NAD^+ (200 μM) and $NAADP^+$ (30–50 μM) triggered similar Ca^{2+} transients in all of them (Fig. 6C), while only one cell generated detectable Ca^{2+} transients on 30 μM NF 546 (Fig. 6C, cell 2). In all these cases, NF 340 inhibited cellular responses to ATP and $NAADP^+$ (Fig. 6D), verifying that just $P2Y_{11}$ mediated MSC responses to these agonists. Because

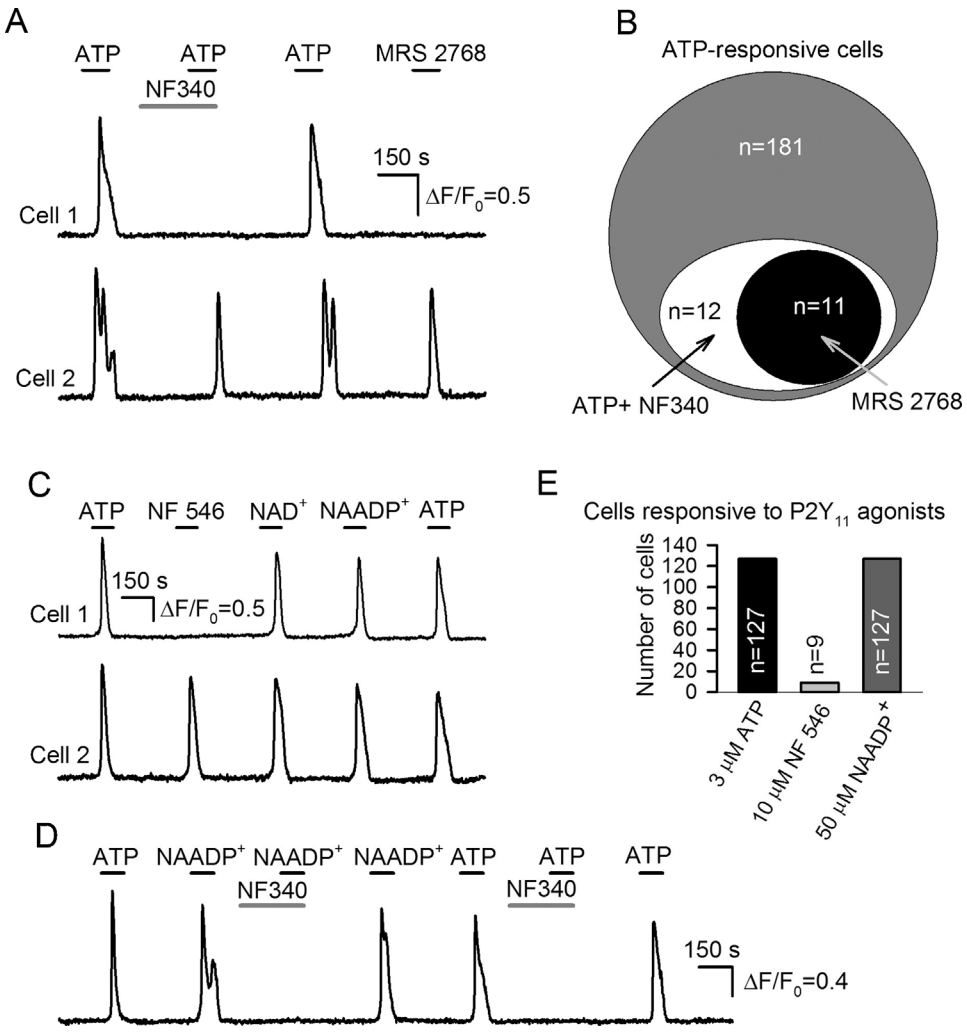

Fig. 6. Sensitivity of MSCs to a variety of purinergic agonists and antagonists. (*A*) Representative responses of 2 concurrently assayed cells to 3 μM ATP and the $P2Y_2$ agonist MRS 2768. Most ATP-sensitive MSCs were rendered nonresponsive by 30 μM NF 340, a $P2Y_{11}$ antagonist, and did not respond to 10 μM MRS 2768 (Cell 1). In rare cells that remained responsive to ATP in the presence of 30 μM NF 340, 10 μM MRS 2768 elicited Ca^{2+} transients (Cell 2). (*B*) Summary of MSC responses to MRS 2768 and ATP responses recorded from 181 cells in control and in the presence of NF 340. (*C*) Representative responses of 2 cells to $P2Y_{11}$ agonists. NAD^+ (200 μM) and $NAADP^+$ (50 μM) elicited Ca^{2+} transients in all assayed ATP-sensitive MSCs (Cell 1) (n = 127), while only few cells (n = 9) responded to 10 μM NF 546, a specific $P2Y_{11}$ agonist (Cell 2). (*D*) $P2Y_{11}$ antagonist NF340 (30 μM) rendered MSCs nonresponsive to both 50 μM $NAADP^+$ and 3 μM ATP-sensitive MSCs (23 cells). (*E*) Summary of MSC responses (127 cells) to 3 μM ATP, 10 μM NF 546, and 50 μM $NAADP^+$ that were applied in series.

NAD^+ also might act via adenosine receptors or by stimulating $P2Y_1$ and some P2X receptors [51–54], much more effective $NAADP^+$ was used in further experiments. Overall, we assayed 127 ATP-sensitive MSCs and found all of them to respond to $NAADP^+$ (30–50 μM) with Ca^{2+} transients (Fig. 6C, D). Altogether, these findings verified that $P2Y_{11}$ is a principal ATP receptor in MSCs. In contrast to the natural $P2Y_{11}$ agonists, 30 μM NF-546 elicited detectable Ca^{2+} bursts only in 9 (7%) out of 127 ATP/$NAADP^+$-responsive cells (Fig. 6C, cell 2; Fig. 6E). At the moment we cannot provide any valid explanation for low efficacy of NF-546 relative to ATP and $NAADP^+$ (Fig. 6E). Perhaps, this synthetic ligand is a biased agonist that enables coupling of $P2Y_{11}$ to the phosphoinositide cascade by involving only a certain G-protein type, which is absent or relatively less abundant in the most of MSCs.

Because MSCs express $P2Y_2$ and $P2Y_4$ (Fig. 2B), a particular cell could employ each or both of these UTP receptors for monitoring extracellular UTP. In dedicated experiments, we identified 95 MSCs responsive to 10 μM UTP with Ca^{2+} transients and analyzed their sensitivity to MRS 2768 and MRS 4062, specific agonists of $P2Y_2$ and $P2Y_4$ receptors, respectively. Consistently with recordings from ATP-responsive cells (Fig. 6B), we found only 9 (9.5%) out of 95 UTP-sensitive cells to respond to 10 μM MRS 2768 (Fig. 7A, cell 3; Fig. 7B). In contrast, 78 cells (82%) responded to 10 μM MRS 4062 (Fig. 7, cell 1; Fig. 7B). These findings suggest that MSCs rely predominantly on $P2Y_4$ to detect extracellular UTP, while $P2Y_2$ is either expressed in a very small subpopulation of $P2Y_4$-negative cells or not coupled to Ca^{2+} mobilization in a great majority of $P2Y_4$-positive cells.

The analysis of ADP responsiveness included 87 MSCs sensitive to 3 μM ADP (Fig. 8A) that was presumably recognized by $P2Y_1$ and/or $P2Y_{13}$ receptors, given that $P2Y_{12}$ transcripts were not found in MSCs (Fig. 2B). To evaluate a role of the $P2Y_1$, we treated 65 ADP-sensitive MSCs with MRS 2365, a highly potent and selective $P2Y_1$ agonist that displays no activity at $P2Y_{12}$ and $P2Y_{13}$ at submicromolar concentrations [55]. When applied at 100–300 nM, MRS 2365 was ineffective but triggered Ca^{2+} signaling in 16 (25%) out of 65 MSCs at 10 μM (Fig. 8A). Because specific effects of MRS 2365 are characterized by EC_{50} ~1 nM [55], this $P2Y_1$ agonist might bring about a nonspecific action at the concentration of 10 μM. On the other hand, MRS 2179 (10 μM), a $P2Y_1$ antagonist with IC_{50} = 0.15 μM [48], inhibited ADP responses in all treated MSCs (65 cells) (Fig. 8A). Given that other P2Y receptors were hardly inhibited by 10 μM MRS 2179 [48], the observed effects of the specific agonist and antagonist of the $P2Y_1$ receptor were rather inconsistent. To reconcile these contradictory findings, we considered the possibility that both $P2Y_1$ and $P2Y_{13}$ should have been active concurrently to stimulate Ca^{2+} signaling in MSCs. If so, nanomolar MRS 2365 was ineffective, activating solely $P2Y_1$, while 10 μM MRS 2365 affected both $P2Y_1$ and $P2Y_{13}$ [55], thus initiating Ca^{2+} signaling in MSCs. This model predicted inability of MSCs to respond to ADP if either $P2Y_1$ or $P2Y_{13}$ was inhibited. In line with this idea, we assayed sensitivity of 46 ADP-responsive MSCs to both MRS 2179 (10 μM) and MRS 2211 (10 μM), a $P2Y_{13}$ antagonist. It turned out that either of these compounds rendered each of 46 assayed cells nonresponsive to ADP (Fig. 8B, C). As a negative control, we treated 14 cells with the $P2Y_{12}$ antagonist clopidogrel (10 μM) and found one to affect ADP responses negligibly (Fig. 8B). Altogether, our findings (Fig. 8A–C) strongly

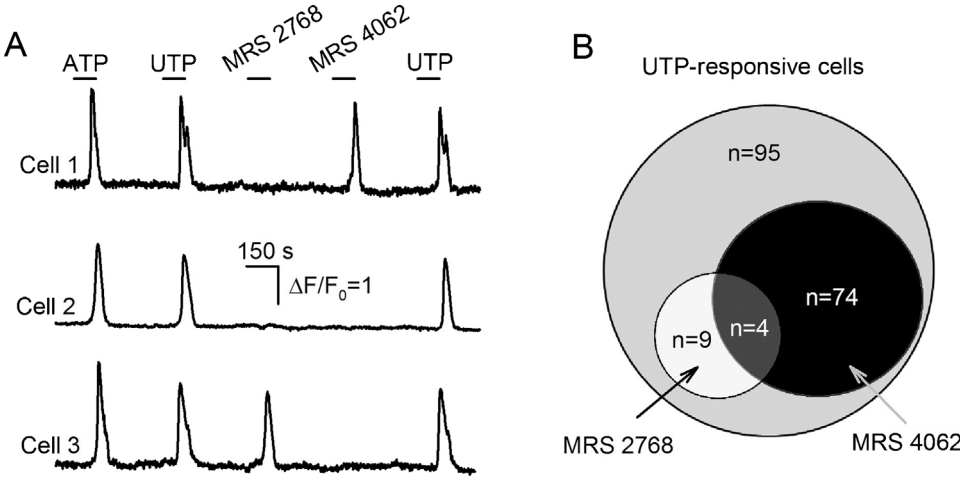

Fig. 7. Sensitivity of UTP-responsive MSCs to $P2Y_2$ and $P2Y_4$ agonists. (*A*) Representative recordings from purinergic MSCs sequentially stimulated by 3 μM ATP and 10 μM UTP as well as by 10 μM MRS 2768 and 10 μM MRS 4062, specific agonists of $P2Y_2$ and $P2Y_2$ receptor, respectively. (*B*) Responsiveness of UTP-sensitive MSCs (n = 95) to MRS 2768 and MRS 4062.

argued that a given MSC was capable of generating robust Ca^{2+} responses to ADP only if both $P2Y_1$ and $P2Y_{13}$ receptors were functional.

It is noteworthy that in overall experiments, we used MSCs isolated from adipose tissues of 15 individuals and found that regardless of a particular donor, primary MSC culture contained similar fractions of cells responsive to ATP, UTP, and/or ADP (Fig. 1). In contrast, only 2 donors provided a cellular material that contained rare UDP-responsive MSCs. The experiments with specific P2Y ligands partly illustrated in Figs. 6-8 were performed with MSCs that were isolated from adipose tissues of 5 donors, including 2 special donors mentioned above. We did not reveal a noticeable donor-dependence of MSC responsiveness to the synthetic agonists and antagonists of ATP, UTP, and ADP receptors. In the case of MSC colonies with rare UDP-sensitive cells, we assayed 726 MSCs in total and found only 15 cells (2%) to respond to 10 μM UDP with Ca^{2+} transients (Fig. 8D). All these UDP-sensitive cells also responded to the $P2Y_6$ agonist MRS 2693 (10 μM) (Fig. 8D), suggesting $P2Y_6$ to be predominantly involved.

4. Discussion

MSCs are capable of sensing complex extracellular cues, including hormones, cytokines, and nucleotides, the capability enabling a necessary adjustment of their physiology to microinviroment specific to a tissue wherein they reside [19]. In the present work, we explored Ca^{2+} signaling initiated by purinergic agonists in MSCs derived from the human adipose tissue (hAD-MSCs). We aimed at the identification of P2Y receptors coupled to Ca^{2+}mobilization in hAD-MSCs and focused on the functional analysis of purinergic transduction. As a rule, we assayed hAD-MSC colonies of 2-4 passages since those were mostly abundant (~11% on average) with cells capable of generating Ca^{2+} transients on bath ATP; in later passages, the fraction of ATP-responsive cells declined. Because the refractory period characteristic of nucleotide responses was lengthy (~400 s), a particular recording usually lasted 40–60 min. During this prolonged assay responsiveness of many cells to P2Y agonists was liable to rundown, thus hampering the quantitative analysis. Given the abovementioned factors and that cellular material was not unlimited, the whole set of experiments described here (Figs. 1–8) could not be accomplished with hAD-MSCs derived from a single donor only. In other words, experiments of the particular type, e.g. the generation of dose-response curves (Fig. 3), were carefully performed using hAD-MSCs derived from a particular donor. Taking into account obtained results, we tried to reproduce most important findings by assaying hAD-MSCs from as many donors as possible. For instance, the hAD-MSC responsivity to ATP and UDP was invariably assayed in all cases, while the expression analysis of purinoreceptors (Fig. 2) involved 7 donors.

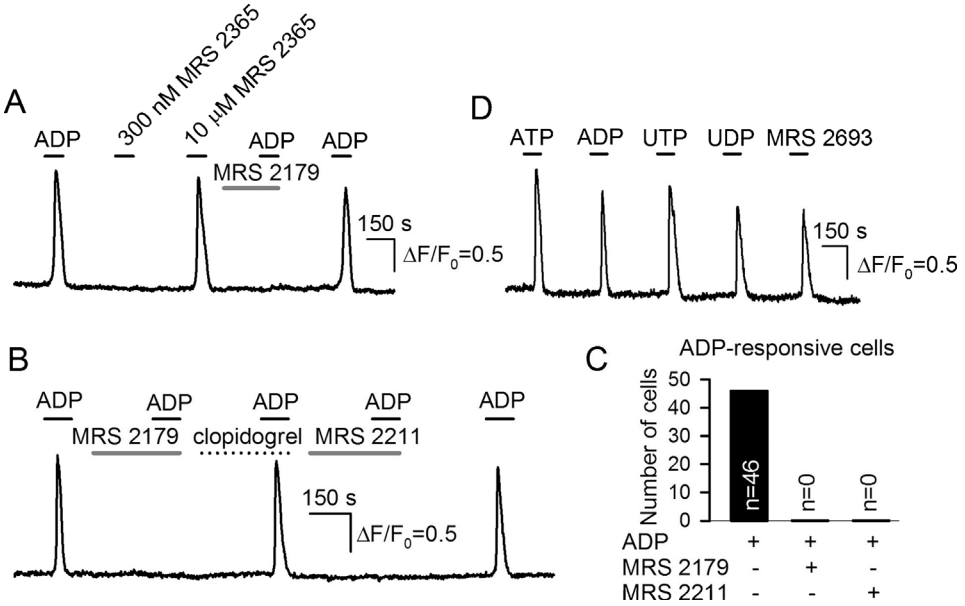

Fig. 8. MSC receptors to ADP and UDP. (*A*) Representative MSC responses to 3 μM ADP and to the $P2Y_1$ agonist MRS 2365 applied at the concentrations of 300 nM and 10 μM. All cells treated with 10 μM MRS 2179 (n = 65) became nonresponsive to 3 μM ADP. (*B*) When applied alone at 10 μM, antagonists of $P2Y_1$ (MRS 2179) and $P2Y_{13}$ (MRS 2211) inhibited responses of MSCs to 3 μM ADP (46 cells). The $P2Y_{13}$ antagonist clopidogrel (10 μM) never affected ADP responses. (*C*) Summary of responses of 46 MSCs to 3 μM ADP in control and in the presence of MRS 2179 and MRS 2211, both being applied at 10 μM ATP. (*D*) Representative recording from MSC responsive to 10 μM UDP (15 cells) that were also sensitive to the $P2Y_6$ agonist MRS 2693 (10 μM).

4.1. Expression analysis of P2 receptor transcripts

We performed the expression analysis of purinoreceptors in hAD-MSCs by using conventional RT-PCR and gene-specific primers. RNA was isolated from two cell preparations that contained UDP-responsive hAD-MSCs and from 5 preparations, wherein UDP-responsive cells were not identified. It turned out that similar sets of P1 and P2 transcripts were identified in all 7 RNA samples. In all cases, we particularly detected transcripts for $P2Y_1$, $P2Y_2$, $P2Y_4$, $P2Y_6$, $P2Y_{11}$, $P2Y_{13}$, and $P2Y_{14}$ (Fig. 2B) but not for $P2Y_{12}$. Reportedly, P2Y receptors are couple to multiple signaling pathways, depending on cellular context [8–11]. Therefore, the ability of a given MSC to generate Ca^{2+} transients on response to P2Y agonists is determined not only by a set of expressed P2Y receptors but also by their coupling to intracellular signaling pathways. Thus, our failure to find UDP-responsive cells in most cellular preparations could be attributed to that $P2Y_6$ and $P2Y_{14}$ are not coupled to Ca^{2+} mobilization in the vast majority of hAD-MSCs.

Previously, the expression of P2 receptors in human MSCs was analyzed largely in bone marrow-derived cells (hBD-MSCs). In earlier reports, the expression of $P2Y_1$ and not-identified P2X receptors in hBD-MSCs has been suggested based on functional evidence [27,33]. The later study of hBD-MSCs revealed transcripts for all eight P2Y receptors and for six P2X receptors, except for $P2X_2$ [56]. Functional, pharmacological, and molecular analysis implicated $P2Y_1$, $P2Y_4$, and P2´7 receptors in modulating differentiation capacity of hBD-MSCs [21,30]. Reportedly, $P2Y_1$, $P2Y_{11}$, $P2X_4$, $P2X_6$, and $P2X_7$ are expressed in dental pulp MSCs [31]. The previous expression analysis of hAD-MSCs revealed transcripts for all P2Y and all P2X receptors [28]. In contrast, we did not detect transcripts for $P2Y_{12}$, $P2X_1$, $P2X_3$, $P2X_5$, and $P2X_6$ receptors (Fig. 3). At the moment we have no plausible explanation for this discrepancy. Note however that for P2Y receptors, our functional findings (FigS. 5–8) correlate well with the molecular data (Fig. 2B). In particular, the negligible effect of the $P2Y_{12}$ antagonist on hAD-MSC responses to ADP (Fig. 8B) is completely consistent with the absence of detectable $P2Y_{12}$ transcripts in our cellular preparations (Fig. 2B).

4.2. MSC responsiveness to purinergic agonists

The responsiveness to ATP, ADP, and UTP was distributed non-uniformly among purinergic hAD-MSCs. Regardless of a particular donor and a passage, ATP was the most effective, while UTP and ADP mobilized Ca^{2+} with lesser efficacy and almost exclusively in ATP-sensitive cells. Cells responsive to ATP/UTP or to ATP/ADP comprised virtually separate subpopulations in a group of purinergic hAD-MSCs. Only nearly one in every ten purinergic cells responded to all three nucleotides (Fig. 1). These findings indicate that expression of a particular P2Y receptor and/or its coupling to Ca^{2+} mobilization varied from cell to cell. The effects of subtype specific agonists and antagonists of P2Y receptors (Figs. 6–8) suggest that $P2Y_{11}$ is a primary ATP receptor in hAD-MSCs, which employ both $P2Y_1$ and $P2Y_{13}$ to detect ADP, while UTP responses are largely mediated by $P2Y_4$. The very uncommon UDP-sensitive hAD-MSCs responded to MRS 2693 invariably (Fig. 8D), suggesting that presumably $P2Y_6$ mediated UDP-dependent Ca^{2+} signals.

Although NAD is largely known as a key player in energy metabolism [57], growing evidence implicates this nucleotide in intracellular and extracellular signaling [58]. In our experiments, oxidized NAD (NAD^+) mobilized Ca^{2+} in each treated ATP-responsive cell (Fig. 6C, D). The responsivity to extracellular NAD^+ is not surprising, given that hAD-MSCs express $P2Y_1$ and $P2Y_{11}$ (Fig. 2B) recognizing NAD^+ as an agonist [49,51,54,59]. In light of the emerging concept on a role of NAD^+ in cell physiology [58,60], it is not unlikely that extracellular NAD^+ serves as an autocrine/paracrine modulator of MSC functions. Indeed, MSCs of different origin can release NAD^+ through Cx43 hemichannels [34,61]. In addition to $P2Y_1$ and $P2Y_{11}$, extracellular NAD^+ also serves as agonist for certain P2X receptors [51,53] and for the A1 adenosine receptor [62]. MSCs express several ectoenzymes, including NAD^+-pyrophosphatase (NPP1) and ecto-5′-nucleotidase (CD73), which could process NAD^+ outside cells [34,63,64]. Extracellular NAD^+ and downstream signaling molecules can exert autocrine and paracrine regulatory effects on MSCs by acting via multiple signaling circuits [34,63,64,65]. For instance, Fruscione and co-authors [34] revealed the autocrine regulatory pathway in hBD-MSCs that includes release of NAD^+ via Cx43 hemichannels, stimulation of $P2Y_{11}$, and activation of the cAMP-cADP-ribose-Ca^{2+} signaling cascade. This circuit presumably controls several important hBD-MSC functions, including proliferation, migration, and secretion of prostaglandin E2 and cytokines. It is not unlikely that a similar regulatory pathway operates in hAD-MSC as well.

4.3. Coupling of P2Y receptors to intracellular signaling pathways

The purinergic transduction in hAD-MSCs involves P2Y receptors that are coupled by the phosphoinositide cascade to Ca^{2+} release from Ca^{2+} stores (Fig. 4). When assayed at multiple ATP concentrations, hAD-MSC responded to the nucleotide in “all-or-nothing” manner (Fig. 3A, B). Although we did not probe other P2Y agonists at widely varied concentrations, presumably, ADP- and UTP-responses also obeyed a step-like dose-dependence. Indeed, at the concentrations of 1 and 30 μM (3 and 50 μM), ADP (UTP) elicited Ca^{2+} transients that were similar by magnitude (Fig. 1S). By using Ca^{2+} uncaging, we demonstrated that Ca^{2+}-induced Ca^{2+} release (CICR) is characteristic of purinergic hAD-MSCs (Fig. 5). Given that MSC responses to ATP and other nucleotides were quite similar kinetically and by magnitude to Ca^{2+} signals associated with CICR (Fig. 5A), we inferred that the purinergic transduction culminates in avalanche-like CICR that equalizes Ca^{2+} signals elicited by P2Y agonists at varied concentrations. By analogy with adrenergic hAD-MSCs [38], we suggest that the purinergic transduction may include two coupled mechanisms. By stimulating P2Y receptors and the downstream phosphoinositide cascade, a P2Y agonist initially produces a small and local Ca^{2+} signal, which then triggers, should it exceed a threshold, a regenerative process mediated by CICR, thus resulting in a global and universal Ca^{2+} response.

It is widely accepted that a population of MSCs from different sources is a heterogeneous mixture of cells, including multipotent and more committed progenitor cells [12,13,35,36]. Yet, cultured MSCs are not synchronized and dwell in different phases of the cell cycle. It therefore might be expected that divergent intracellular signaling is inherent in a MSC population, containing both proliferating and quiescent cells. The abovementioned factors could underlie functional heterogeneity of a MSC population discussed previously [35,36,38]. In our experiments, ATP and other P2Y agonists elicited detectable Ca^{2+} signals in a small (12-15%) fraction of hAD-MSCs. Perhaps, P2Y receptors were not expressed or coupled to Ca^{2+} mobilization in a majority of hAD-MSCs assayed here. Given that the pharmacological evidence (Fig. 6) pointed at $P2Y_{11}$ as a principal ATP receptor in hAD-MSCs, we attempted to correlate ATP responsivity and expression of $P2Y_{11}$ receptors. When hAD-MSC samples (n = 3) were treated with rabbit antibody recognizing the human $P2Y_{11}$ protein, a majority (73 ± 4%) of stained cells exhibited $P2Y_{11}$-like immunoreactivity (Fig. 9A), exceeding a fraction of ATP-responsive cells (~11%) by several folds. It thus appears that most of $P2Y_{11}$-positive hAD-MSCs are unable to generate global Ca^{2+} signals in response to ATP. Perhaps, in many cells expressing $P2Y_{11}$, ATP transduction did not involve Ca^{2+} signaling as such. Indeed, $P2Y_{11}$ regulates PLCβ, ion channels, PI3 kinase, RGS, and some other signaling proteins by engaging G_q/G_{11} [66] and stimulates adenylyl cyclase via G_s [67]. Alternatively, coupling of $P2Y_{11}$ to Ca^{2+} mobilization might not take place in irresponsive hAD-MSCs because downstream machinery failed. Note that in our experiments, Ca^{2+} uncaging elicited agonist-like Ca^{2+} responses (Fig. 5A) in a nearly 12% fraction of hAD-MSCs loaded with NP-EGTA (411 cells). Perhaps, the CICR mechanism was disabled in many assayed hAD-

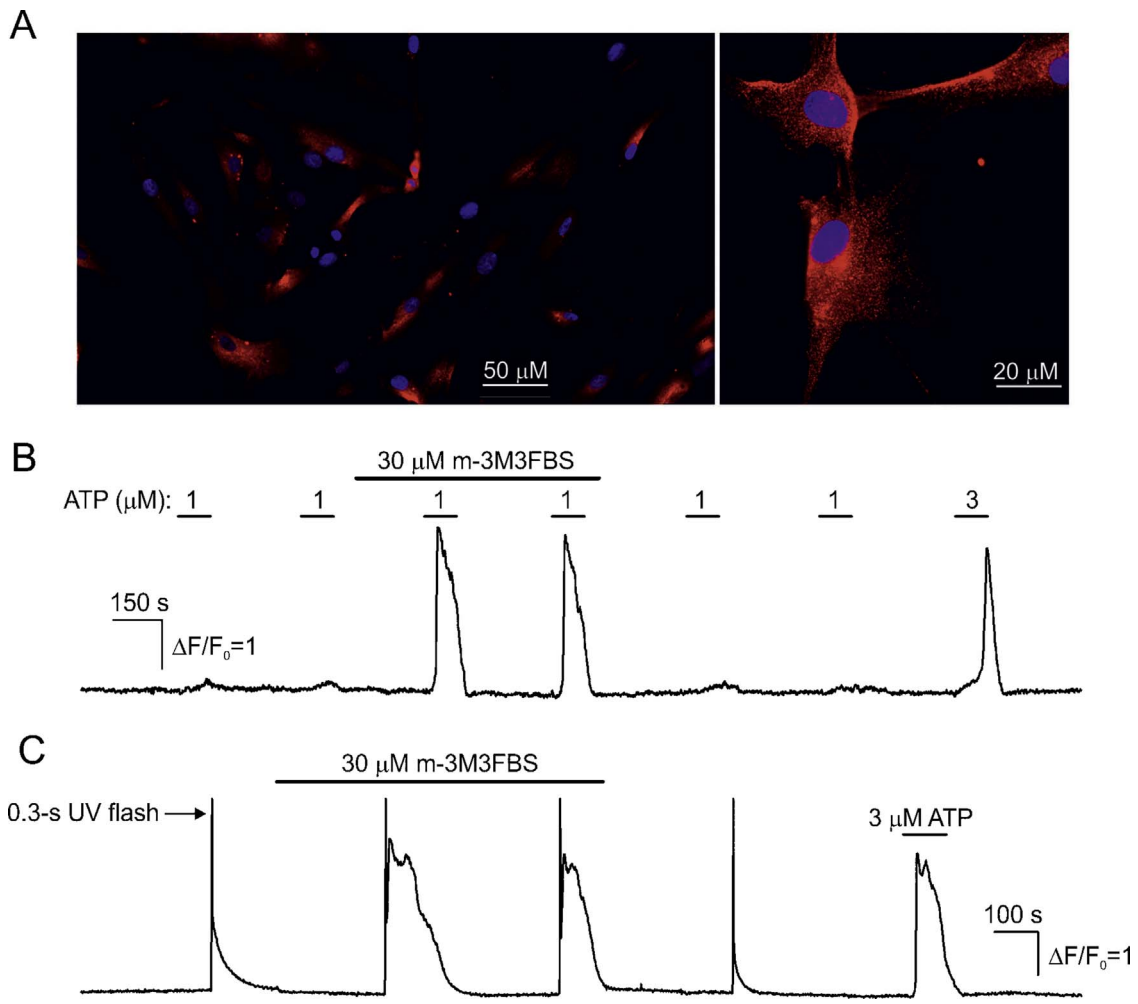

Fig. 9. Detection of the $P2Y_{11}$ protein in hAD-MSC. (*A*) Fluorescent images of a MCS colony treated with rabbit antibody against the human $P2Y_{11}$ protein and goat anti-rabbit IgG labeled with AlexaFluor 594. Excitation − 570 ± 15 nm, emission − 630 ± 30 nm. In the left and right panels, magnification was 20 × and 63 × , respectively. (*B*, *C*) PLC activator m-3M3FBS enhances MSC sensitivity to both ATP and Ca^{2+} uncaging. Two different cells were assayed in (*B*) and (*C*).

MSCs, thereby making cells irresponsive, in terms of global Ca^{2+} signaling, to ATP and other purinergic agonists.

The CICR mechanism involves IP_3- and/or ryanodine receptors active in a Ca^{2+} store that is sufficiently filled with Ca^{2+} ions. Our physiological evidence implicates basically IP_3 receptors in mediating both purinergic transduction and CICR, suggesting a negligible contribution of ryanodine receptors to these processes (Figs. 4 C and 5 C). The CICR mechanism might be disabled in irresponsive hAD-MSCs for several reasons. In particular, an IP_3 level at rest might be too low to mediate sufficient sensitivity of IP_3 receptors to cytosolic Ca^{2+}. Alternatively, releasable Ca^{2+}pool might be insufficient due to increased leakage and/or scanty activity of reticular Ca^{2+}-ATPase to provide global Ca^{2+} signaling. In some experiments, we attempted to elucidate whether a resting IP_3 level could influence CICR in hAD-MSCs and their sensitivity to ATP. To shift equilibrium between production and hydrolysis of IP_3 in resting cells, we used the membrane-permeable PLC activator m-3M3FBS. By suggesting that a threshold concentration of an agonist depends on a resting IP_3 level, we focused on cells (n = 11) that exhibited relatively low sensitivity and did not respond to 1 μM ATP (Fig. 9B). The addition of 30 μM m-3M3FBS to the bath rendered most (n = 7) of these cells responsive to 1 μM ATP but they became non-responsive again after removal of this PLC activator (Fig. 9A). Moreover, in a number of cells (n = 5), wherein Ca^{2+} uncaging produced by 0.3-s UV pulses did not stimulate CICR, light flashes elicited ATP response-like Ca^{2+} signals associated with CICR, provided that 30 μM m-3M3FBS was present in the bath (Fig. 9C). Thus, these preliminary experiments support the idea that a resting IP_3 level can influence cell sensitivity to ATP, presumably by determining a threshold level of intracellular Ca^{2+} capable of bursting into CICR. Further experiments are required to elucidate whether other factors, including a low level of Ca^{2+} in the lumen of the endoplasmic reticulum, might underlie a failure of global Ca^{2+} signaling in hAD-MSCs nonresponsive to P2Y agonists.

Conflict of interest

No conflict of interest is declared by the authors.

Acknowledgments

This work was supported by the Russian Science Foundation (grant 17-75-10127).

Appendix A. Supplementary data

Supplementary data associated with this article can be found, in the online version, at http://dx.doi.org/10.1016/j.ceca.2017.11.001.

References

[1] G. Burnstock, Purinergic signalling: from discovery to current developments, Exp. Physiol. 99 (2014) 16–34.

[2] A. Verkhratsky, G. Burnstock, Biology of purinergic signalling: its ancient evolutionary roots, its omnipresence and its multiple functional significance, BioEssays 36 (2014) 697–705.
[3] H. Zimmermann, M. Zebisch, N. Strater, Cellular function and molecular structure of ecto-nucleotidases, Purinergic Signal. 8 (2012) 437–502.
[4] B.B. Fredholm, A.P. IJzerman, K.A. Jacobson, J. Linden, C.E. Muller, International Union of Basic and Clinical Pharmacology. LXXXI. Nomenclature and classification of adenosine receptors–an update, Pharmacol. Rev. 63 (2011) 1–34.
[5] R.D. Fields, G. Burnstock, Purinergic signalling in neuron-glia interactions, Nat. Rev. Neurosci. 7 (2006) 423–436.
[6] D.S. Samways, Z. Li, T.M. Egan, Principles and properties of ion flow in P2X receptors, Front. Cell. Neurosci. 8 (2014) 6.
[7] A. Saul, R. Hausmann, A. Kless, A. Nicke, Heteromeric assembly of P2X subunits, Front. Cell. Neurosci. 7 (2013) 250.
[8] S. Buvinic, R. Briones, J.P. Huidobro-Toro, $P2Y_1$ and $P2Y_2$ receptors are coupled to the NO/cGMP pathway to vasodilate the rat arterial mesenteric bed, Br. J. Pharmacol. 136 (2002) 847–856.
[9] T.M. Luke, T.D. Hexum, UTP and ATP increase extracellular signal-regulated kinase 1/2 phosphorylation in bovine chromaffin cells through epidermal growth factor receptor transactivation, Purinergic Signal. 4 (2008) 323–330.
[10] C. Malaval, M. Laffargue, R. Barbaras, C. Rolland, C. Peres, E. Champagne, B. Perret, F. Terce, X. Collet, L.O. Martinez, RhoA/ROCK I signalling downstream of the $P2Y_{13}$ ADP-receptor controls HDL endocytosis in human hepatocytes, Cell. Signal. 21 (2009) 120–127.
[11] M. Montiel, E.P. de la Blanca, E. Jimenez, P2Y receptors activate MAPK/ERK through a pathway involving PI3 K/PDK1/PKC-zeta in human vein endothelial cells, Cell. Physiol. Biochem. 18 (2006) 123–134.
[12] P.C. Baer, Adipose-derived mesenchymal stromal/stem cells: An update on their phenotype in vivo and in vitro, World J. Stem Cells 6 (2014) 256–265.
[13] N.I. Kalinina, V.Y. Sysoeva, K.A. Rubina, Y.V. Parfenova, V.A. Tkachuk, Mesenchymal stem cells in tissue growth and repair, Acta Naturae 3 (2011) 30–37.
[14] A. Keating, Mesenchymal stromal cells: new directions, Cell Stem Cell 10 (2012) 709–716.
[15] R.R. Sharma, K. Pollock, A. Hubel, D. McKenna, Mesenchymal stem or stromal cells: a review of clinical applications and manufacturing practices, Transfusion 54 (2014) 1418–1437.
[16] F. Cavaliere, C. Donno, N. D'Ambrosi, Purinergic signaling: a common pathway for neural and mesenchymal stem cell maintenance and differentiation, Front. Cell. Neurosci. 9 (2015) 211.
[17] O. Forostyak, S. Forostyak, S. Kortus, E. Sykova, A. Verkhratsky, G. Dayanithi, Physiology of Ca^{2+} signalling in stem cells of different origins and differentiation stages, Cell Calcium 59 (2016) 57–66.
[18] T. Glaser, A.R. Cappellari, M.M. Pillat, I.C. Iser, M.R. Wink, A.M. Battastini, H. Ulrich, Perspectives of purinergic signaling in stem cell differentiation and tissue regeneration, Purinergic Signal. 8 (2012) 523–537.
[19] S. Scarfi, Purinergic receptors and nucleotide processing ectoenzymes: Their roles in regulating mesenchymal stem cell functions, World J. Stem Cells 6 (2014) 153–162.
[20] L.H. Jiang, Y. Hao, F. Mousawi, H. Peng, X. Yang, Expression of P2 purinergic receptors in mesenchymal stem cells and their roles in extracellular nucleotide regulation of cell functions, J. Cell. Physiol. 232 (2017) 287–297.
[21] M. Ciciarello, R. Zini, L. Rossi, V. Salvestrini, D. Ferrari, R. Manfredini, R.M. Lemoli, Extracellular purines promote the differentiation of human bone marrow-derived mesenchymal stem cells to the osteogenic and adipogenic lineages, Stem Cells Dev. 22 (2013) 1097–1111.
[22] B. Gharibi, A.A. Abraham, J. Ham, B.A. Evans, Contrasting effects of A1 and A2b adenosine receptors on adipogenesis, Int. J. Obes. (Lond.) 36 (2012) 397–406.
[23] B.A. Evans, C. Elford, A. Pexa, K. Francis, A.C. Hughes, A. Deussen, J. Ham, Human osteoblast precursors produce extracellular adenosine, which modulates their secretion of IL-6 and osteoprotegerin, J. Bone Miner. Res. 21 (2006) 228–236.
[24] S.H. Carroll, N.A. Wigner, N. Kulkarni, H. Johnston-Cox, L.C. Gerstenfeld, K. Ravid, A2 B adenosine receptor promotes mesenchymal stem cell differentiation to osteoblasts and bone formation in vivo, The J. Biol. Chem. 287 (2012) 15718–15727.
[25] B. Gharibi, A.A. Abraham, J. Ham, B.A. Evans, Adenosine receptor subtype expression and activation influence the differentiation of mesenchymal stem cells to osteoblasts and adipocytes, J. Bone Miner. Res. 26 (2011) 2112–2124.
[26] W. He, A. Mazumder, T. Wilder, B.N. Cronstein, Adenosine regulates bone metabolism via A1, A2A, and A2 B receptors in bone marrow cells from normal humans and patients with multiple myeloma, FASEB J. 27 (2013) 3446–3454.
[27] S. Kawano, K. Otsu, A. Kuruma, S. Shoji, E. Yanagida, Y. Muto, F. Yoshikawa, Y. Hirayama, K. Mikoshiba, T. Furuichi, ATP autocrine/paracrine signaling induces calcium oscillations and NFAT activation in human mesenchymal stem cells, Cell Calcium 39 (2006) 313–324.
[28] N. Zippel, C.A. Limbach, N. Ratajski, C. Urban, C. Luparello, A. Pansky, M.U. Kassack, E. Tobiasch, Purinergic receptors influence the differentiation of human mesenchymal stem cells, Stem Cells Dev. 21 (2012) 884–900.
[29] J.B. Noronha-Matos, J. Coimbra, A. Sa-e-Sousa, R. Rocha, J. Marinhas, R. Freitas, S. Guerra-Gomes, F. Ferreirinha, M.A. Costa, P. Correia-de-Sa, P2X7-induced zeiosis promotes osteogenic differentiation and mineralization of postmenopausal bone marrow-derived mesenchymal stem cells, FASEB J. 28 (2014) 5208–5222.
[30] D. Sun, W.G. Junger, C. Yuan, W. Zhang, Y. Bao, D. Qin, C. Wang, L. Tan, B. Qi, D. Zhu, X. Zhang, T. Yu, Shockwaves induce osteogenic differentiation of human mesenchymal stem cells through ATP release and activation of P2X7 receptors, Stem Cells (Dayton, Ohio) 31 (2013) 1170–1180.
[31] H. Peng, Y. Hao, F. Mousawi, S. Roger, J. Li, J.A. Sim, S. Ponnambalam, X. Yang, L.H. Jiang, Purinergic and store-operated Ca^{2+} signaling mechanisms in mesenchymal stem cells and their roles in ATP-induced stimulation of cell migration, Stem Cells (Dayton, Ohio) 34 (2016) 2102–2114.
[32] G. Biver, N. Wang, A. Gartland, I. Orriss, T.R. Arnett, J.M. Boeynaems, B. Robaye, Role of the $P2Y_{13}$ receptor in the differentiation of bone marrow stromal cells into osteoblasts and adipocytes, Stem Cells (Dayton, Ohio) 31 (2013) 2747–2758.
[33] E. Coppi, A.M. Pugliese, S. Urbani, A. Melani, E. Cerbai, B. Mazzanti, A. Bosi, R. Saccardi, F. Pedata, ATP modulates cell proliferation and elicits two different electrophysiological responses in human mesenchymal stem cells, Stem Cells (Dayton, Ohio) 25 (2007) 1840–1849.
[34] F. Fruscione, S. Scarfi, C. Ferraris, S. Bruzzone, F. Benvenuto, L. Guida, A. Uccelli, A. Salis, C. Usai, E. Jacchetti, C. Ilengo, S. Scaglione, R. Quarto, E. Zocchi, A. De Flora, Regulation of human mesenchymal stem cell functions by an autocrine loop involving NAD^+ release and $P2Y_{11}$-mediated signaling, Stem Cells Dev. 20 (2011) 1183–1198.
[35] J. Galle, M. Hoffmann, A. Krinner, Mesenchymal stem cell heterogeneity and ageing in vitro: a model approach, in: L. Geris (Ed.), Computational Modeling in Tissue Engineering, Springer, Berlin Heidelberg, 2013, pp. 183–205.
[36] D.G. Phinney, Functional heterogeneity of mesenchymal stem cells: implications for cell therapy, J. Cell. Biochem. 113 (2012) 2806–2812.
[37] P.A. Zuk, M. Zhu, H. Mizuno, J. Huang, J.W. Futrell, A.J. Katz, P. Benhaim, H.P. Lorenz, M.H. Hedrick, Multilineage cells from human adipose tissue: implications for cell-based therapies, Tissue Eng. 7 (2001) 211–228.
[38] P.D. Kotova, V.Y. Sysoeva, O.A. Rogachevskaja, M.F. Bystrova, A.S. Kolesnikova, P.A. Tyurin-Kuzmin, J.I. Fadeeva, V.A. Tkachuk, S.S. Kolesnikov, Functional expression of adrenoreceptors in mesenchymal stromal cells derived from the human adipose tissue, Biochim. Biophys. Acta 1843 (2014) 1899–1908.
[39] N. Kalinina, D. Kharlampieva, M. Loguinova, I. Butenko, O. Pobeguts, A. Efimenko, L. Ageeva, G. Sharonov, D. Ischenko, D. Alekseev, O. Grigorieva, V. Sysoeva, K. Rubina, V. Lazarev, V. Govorun, Characterization of secretomes provides evidence for adipose-derived mesenchymal stromal cells subtypes, Stem Cell Res. Ther. 6 (2015) 221.
[40] G. Burnstock, Purine and pyrimidine receptors, Cell. Mol. Life Sci.: CMLS 64 (2007) 1471–1483.
[41] A. Surprenant, R.A. North, Signaling at purinergic P2X receptors, Annu. Rev. Physiol. 71 (2009) 333–359.
[42] M.J. Berridge, M.D. Bootman, H.L. Roderick, Calcium signalling: dynamics, homeostasis and remodelling, Nat. Rev. Mol. Cell Biol. 4 (2003) 517–529.
[43] S.Z. Xu, F. Zeng, G. Boulay, C. Grimm, C. Harteneck, D.J. Beech, Block of TRPC5 channels by 2-aminoethoxydiphenyl borate: a differential, extracellular and voltage-dependent effect, Br. J. Pharmacol. 145 (2005) 405–414.
[44] T. Mustafa, J. Walsh, M. Grimaldi, L.E. Eiden, PAC1hop receptor activation facilitates catecholamine secretion selectively through 2-APB-sensitive Ca^{2+} channels in PC12 cells, Cell. Signal. 22 (2010) 1420–1426.
[45] C. Harteneck, M. Gollasch, Pharmacological modulation of diacylglycerol-sensitive TRPC3/6/7 channels, Curr. Pharm. Biotechnol. 12 (2011) 35–41.
[46] E.M. Kawamoto, C. Vivar, S. Camandola, Physiology and pathology of calcium signaling in the brain, Front. Pharmacol. 3 (2012) 61.
[47] G.L. Waldo, T.K. Harden, Agonist binding and Gq-stimulating activities of the purified human P2Y1 receptor, Mol. Pharmacol. 65 (2004) 426–436.
[48] I. von Kugelgen, K. Hoffmann, Pharmacology and structure of P2Y receptors, Neuropharmacology 104 (2016) 50–61.
[49] I. Moreschi, S. Bruzzone, R.A. Nicholas, F. Fruscione, L. Sturla, F. Benvenuto, C. Usai, S. Meis, M.U. Kassack, E. Zocchi, A. De Flora, Extracellular NAD^+ is an agonist of the human P2Y11 purinergic receptor in human granulocytes, J. Biol. Chem. 281 (2006) 31419–31429.
[50] I. Moreschi, S. Bruzzone, N. Bodrato, C. Usai, L. Guida, R.A. Nicholas, M.U. Kassack, E. Zocchi, A. De Flora, NAADP$^+$ is an agonist of the human $P2Y_{11}$ purinergic receptor, Cell Calcium 43 (2008) 344–355.
[51] E. Alefishat, S.P. Alexander, V. Ralevic, Effects of NAD at purine receptors in isolated blood vessels, Purinergic Signal. 11 (2015) 47–57.
[52] G. Burnstock, C.H. Hoyle, Actions of adenine dinucleotides in the guinea-pig taenia coli: NAD acts indirectly on P1-purinoceptors; NADP acts like a P2-purinoceptor agonist, Br. J. Pharmacol. 84 (1985) 825–831.
[53] A. Grahnert, C. Klein, S. Hauschildt, Involvement of P2X receptors in the NAD (+)-induced rise in $[Ca^{2+}]_i$ in human monocytes, Purinergic Signal. 5 (2009) 309–319.
[54] C. Klein, A. Grahnert, A. Abdelrahman, C.E. Muller, S. Hauschildt, Extracellular NAD^+ induces a rise in $[Ca^{2+}]_i$ in activated human monocytes via engagement of $P2Y_1$ and $P2Y_{11}$ receptors, Cell Calcium 46 (2009) 263–272.
[55] M. Chhatriwala, R.G. Ravi, R.I. Patel, J.L. Boyer, K.A. Jacobson, T.K. Harden, Induction of novel agonist selectivity for the ADP-activated $P2Y_1$ receptor versus the ADP-activated $P2Y_{12}$ and $P2Y_{13}$ receptors by conformational constraint of an ADP analog, J. Pharmacol. Exp. Ther. 311 (2004) 1038–1043.
[56] D. Ferrari, S. Gulinelli, V. Salvestrini, G. Lucchetti, R. Zini, R. Manfredini, L. Caione, W. Piacibello, M. Ciciarello, L. Rossi, M. Idzko, S. Ferrari, F. Di Virgilio, R.M. Lemoli, Purinergic stimulation of human mesenchymal stem cells potentiates their chemotactic response to CXCL12 and increases the homing capacity and production of proinflammatory cytokines, Exp. Hematol. 39 (2011) 360–374.
[57] E. Verdin, NAD^+ in aging, metabolism, and neurodegeneration, Science (New York, N.Y.) 350 (2015) 1208–1213.
[58] A. Nikiforov, V. Kulikova, M. Ziegler, The human NAD metabolome: Functions, metabolism and compartmentalization, Crit. Rev. Biochem. Mol. Biol. 50 (2015) 284–297.
[59] N.S. Umapathy, E.A. Zemskov, J. Gonzales, B.A. Gorshkov, S. Sridhar, T. Chakraborty, R. Lucas, A.D. Verin, Extracellular beta-nicotinamide adenine dinucleotide (beta-NAD) promotes the endothelial cell barrier integrity via PKA- and EPAC1/Rac1-dependent actin cytoskeleton rearrangement, J. Cell. Physiol. 223

(2010) 215–223.
[60] A. Grahnert, A. Grahnert, C. Klein, E. Schilling, J. Wehrhahn, S. Hauschildt, Review NAD$^+$ a modulator of immune functions, Innate Immunity 17 (2011) 212–233.
[61] A. De Flora, E. Zocchi, L. Guida, L. Franco, S. Bruzzone, Autocrine and paracrine calcium signaling by the CD38/NAD$^+$/cyclic ADP-ribose system, Ann. N. Y. Acad. Sci. 1028 (2004) 176–191.
[62] G.D. Wang, X.Y. Wang, S. Liu, Y. Xia, F. Zou, M. Qu, B.J. Needleman, D.J. Mikami, J.D. Wood, beta-Nicotinamide adenine dinucleotide acts at prejunctional adenosine A1 receptors to suppress inhibitory musculomotor neurotransmission in guinea pig colon and human jejunum, Am. J. Physiol. 308 (2015) G955–963.
[63] S. Scarfì, C. Ferraris, F. Fruscione, C. Fresia, L. Guida, S. Bruzzone, C. Usai, A. Parodi, E. Millo, A. Salis, G. Burastero, A. De Flora, E. Zocchi, Cyclic ADP-ribose-mediated expansion and stimulation of human mesenchymal stem cells by the plant hormone abscisic acid, Stem Cells (Dayton, Ohio) 26 (2008) 2855–2864.
[64] R. Tao, H.Y. Sun, C.P. Lau, H.F. Tse, H.C. Lee, G.R. Li, Cyclic ADP ribose is a novel regulator of intracellular Ca^{2+} oscillations in human bone marrow mesenchymal stem cells, J. Cell. Mol. Med. 15 (2011) 2684–2696.
[65] L. Rossi, V. Salvestrini, D. Ferrari, F. Di Virgilio, R.M. Lemoli, The sixth sense: hematopoietic stem cells detect danger through purinergic signaling, Blood 120 (2012) 2365–2375.
[66] K.B. Hubbard, J.R. Hepler, Cell signalling diversity of the Gqalpha family of heterotrimeric G proteins, Cell. Signal. 18 (2006) 135–150.
[67] B. Torres, A.C. Zambon, P.A. Insel, $P2Y_{11}$ receptors activate adenylyl cyclase and contribute to nucleotide-promoted cAMP formation in MDCK-D1 cells. A mechanism for nucleotide-mediated autocrine-paracrine regulation, J. Biol. Chem. 277 (2002) 7761–7765.